https://doi.org/10.5194/hess-2024-11
Preprint. Discussion started: 23 January 2024

Hydrology and Earth System Sciences
Discussions
Open Access
EGU

Spatiotemporal responses of runoff to climate change on the southern Tibetan Plateau

He Sun[1*], Tandong Yao[1,2], Fengge Su[1,2*], Wei Yang[1,2], Deliang Chen[3]

[1]State Key Laboratory of Tibetan Plateau Earth System, Environment and Resources (TPESER), Institute of Tibetan Plateau Research, Chinese Academy of Sciences, Beijing 100101, China

[2]University of Chinese Academy of Sciences, Beijing 100101, China

[3]Regional Climate Group, Department of Earth Sciences, University of Gothenburg, Gothenburg 405 30, Sweden

*Corresponding author: He Sun, Fengge Su

State Key Laboratory of Tibetan Plateau Earth System, Resources and Environment, Institute of Tibetan Plateau Research, Chinese Academy of Sciences, Beijing 100101, China

Email: sunhe@itpcas.ac.cn, fgsu@itpcas.ac.cn

https://doi.org/10.5194/hess-2024-11
Preprint. Discussion started: 23 January 2024

Hydrology and Earth System Sciences
Discussions
Open Access
EGU

Abstract

A comprehensive understanding of spatiotemporal runoff changes at a sub-basin scale of the Yarlung Zangbo (YZ) basin on the southern Tibetan Plateau (TP), amidst varying climatic and cryospheric conditions, is imperative for effective water resources management. However, spatiotemporal differences of runoff composition, change and the attribution within the YZ basin have not been extensively explored, primarily due to the lack of hydrometeorological observations, especially in the downstream region. In this study, we investigated historical and future evolution of annual and seasonal total water availability, as well as glacier runoff and snowmelt contributions across six sub-basins of the YZ with a particular focus on the comparison between the upstream Nuxia (NX) basin and the downstream Nuxia-Pasighat (NX-BXK) basin, based on a newly generated precipitation dataset and a well-validated model with streamflow, glacier mass, and snow cover observations. Our findings revealed large spatiotemporal differences in changes exist within the YZ basin for 1971–2020. Firstly, runoff generation was dominated by rainfall runoff throughout the YZ basin, with glacier runoff playing more important role in the annual total runoff (19%) in the NX-BXK sub-basin compared to other sub-basins. Notably, glacier runoff contributed 52% of the total runoff at the Pasighat outlet of the YZ basin. Secondly, annual runoff exhibited an increasing trend in the NX basin but a decreasing trend in the NX-BXK, primarily attributed to rainfall runoff changes influenced by atmospheric moisture. Glacier runoff enhanced water supply, by offsetting the decreasing contribution from rainfall. Total runoff will consistently increase

https://doi.org/10.5194/hess-2024-11
Preprint. Discussion started: 23 January 2024


Hydrology and Earth System Sciences
Discussions

(27–100 mm/10yr) across the sub-basins through the 21st century, resulting from increased rainfall runoff and a minor effect of increased snowmelt and glacier runoff.

Keywords

Runoff Composition; Runoff Changes; VIC-Glacier Hydrological Model; Yarlung Zangbo; Tibetan Plateau

Highlights

- Runoff generation is dominated by rainfall runoff (59%–72%) in the YZ, and the largest glacier runoff contribution is in the downstream sub-basin (16%–19%).
- Annual runoff trends indicate an increase in the NX but a decrease in the NX-BXK for 1971–2020, due to contrasting precipitation changes.
- Total runoff across the sub-basins will consistently increase (27–100 mm/10yr) through the 21st century, mostly resulting from increased rainfall runoff.

https://doi.org/10.5194/hess-2024-11
Preprint. Discussion started: 23 January 2024


Hydrology and Earth System Sciences
Discussions

1 Introduction

Climatic and cryospheric changes have profoundly affected hydrological processes in high-mountain regions. The Tibetan Plateau (TP), konwn as the Asian Water Tower, supplying freshwater to nearly 2 billion people. Marked atmospheric warming since the 1980s has changed the balance between liquid and solid states of water, leading to shifts in river runoff, glacier, and snow melt dynamics (Yao et al. 2022). These drastic changes in the upper mountains of the TP pose a threat to the sustainability of the downstream water supply.

The Yarlung Zangbo (YZ, Figure 1) river basin, located in the southern TP is the largest river basin of the TP and a vital freshwater source for the Tibet Autonomous Region (TAR). It constitutes the main agricultural region in the TAR (Yang et al., 1989; Zhong et al., 2014). Like elsewhere on TP, a rapid ongoing temperature rise (0.3–0.4°C per decade) since the mid-1960s potentially influences runoff processes and water resources availability in the YZ basin (Yao et al., 2012; Li et al., 2018). The YZ basin, spanning approximately 250,000 km², exhibits diverse climatic systems, including the Indian summer monsoon and the westerly system, and varying glacier and snow conditions (Zhang et al., 2013). These factors contribute to spatiotemporal differences in runoff changes within the YZ basin. Therefore, gaining a comprehensive understanding of runoff regimes and flow changes at the sub-basin scale is crucial for informed decision-making in water resources management and social development.

https://doi.org/10.5194/hess-2024-11
Preprint. Discussion started: 23 January 2024


Hydrology and Earth System Sciences
Discussions
Open Access
EGU

While numerous studies have investigated runoff regimes and changes using hydrological models in the YZ basin, most have focused solely on the region upstream of the Nuxia (NX) hydrological station (Figure 1) (Chen et al., 2017; Cuo et al., 2019; Su et al., 2016; Zhang et al., 2013; Zhao et al., 2019; Cui et al., 2023; Gu et al., 2023). This focus is due to the nearest national hydrological station's proximity to the mainstream outlet, providing long-term daily records (> 50years). Conversely, the glacierized downstream region (about 65% of the total glacier area in the YZ), particularly between NX and Pasighat outlet (NX-BXK, Figure 1) has received less attention. This lack of focus is attributed to limited hydrometeorological and glacier observations in this sub-basin. Remarkably, this region exhibits the largest glacier retreat in the TP, with a length reduction rate of 48.2m yr^{-1} and an area decrease of 0.57% yr^{-1} during the 1970s–2000s (Yang et al., 2013; Yao et al., 2012). These changes have the potential to significantly alter the runoff regime, influencing the quantity, timing, and variability of flows across space and time. However, the characteristics and changes in runoff, along with the effect of glacier melt on water supply, remain unclear in the NX-BXK sub-basin.

The NX basin, with an area of approximately 201,548 km^2, presents divergent glacier and snow conditions (Table 2). For example, the region upstream of the Lhatse hydrological station (Figure 1), the source region of the YZ river, is influenced by both monsoon and westerlies, experiencing higher precipitation in spring and winter compared to other NX sub-basins (Figure S1 in Supporting Information). The Lhasa (LS) and Rikaze (RKZ) sub-basins,

https://doi.org/10.5194/hess-2024-11
Preprint. Discussion started: 23 January 2024


Hydrology and Earth System Sciences
Discussions

vital crop centers for the central Tibet Autonomous Region, play a crucial role in irrigation water resources. The LS sub-basin, with about 23% snow cover contrasts with the RKZ sub-basin, which has little glacier and snow coverage (Table 2). This difference suggests that the water supply in the RKZ sub-basin is more sensitive to climate change. Moreover, runoff in the region between Yangcun and NX hydrological stations (YC-NX, Figure 1) contributes 51% to the total runoff at the NX hydrological station (Sun and Su, 2020), making runoff regimes and changes in this sub-basin influential for the entire NX basin. Therefore, a comprehensive investigation into runoff regimes and changes in different sub-basins is essential for a nuanced understanding of the mechanisms underlying runoff changes in response to climate change.

While many hydrological studies focus on the region upstream of the NX hydrological station (Zhang et al., 2013; Lutz et al., 2014; Zhao et al., 2019; Sun and Su, 2020; Khanal et al., 2021; Nan et al., 2021; Wang et al., 2021), considerable differences in runoff regimes and change studies exist in the NX basin (Table 1). These differences may arise from variations in forcing inputs for hydrological model simulations. Accurate precipitation inputs play an important role in reliable hydrological model simulations. However, high mountain precipitation in the YZ basin is still inadequately represented in gauge-based, satellite-based, and reanalysis-based estimates, or outputs of regional climate models (Wang and Zeng, 2012; Liu et al., 2020; Sun et al., 2021). The mean annual precipitation ranges from 360–1236 mm in the YZ basin (Qi et al. 2018; Sun; Su 2020; Tong et al. 2014), resulting in significant uncertainties in

https://doi.org/10.5194/hess-2024-11
Preprint. Discussion started: 23 January 2024


Hydrology and Earth System Sciences
Discussions

hydrological simulations. This inconsistency in gridded datasets is often underestimated in hydro-climate studies, especially in glacierized basins with limited data coverage. Even when realistic runoff simulations are achieved at the catchment outlet, they cannot guarantee reasonable results (Zhao et al., 2019) due to the compensation between precipitation-induced runoff and snow/glacier melting. For example, Lutz et al. (2014) simulated glacier runoff in the NX basin with the Spatial Processes in HYdrology (SPHY) model driven by the Asian Precipitation-Highly-Resolved Observational Data Integration Towards Evaluation (APHRODITE) precipitation estimates, suggesting that glacier runoff contributed about 16% to total runoff. In contrast, Khanal et al. (2021) proposed that glacier runoff contributed about 1.8% to total runoff with the same model driven by the newly released fifth-generation reanalysis (ERA5) precipitation of the European Centre for Medium-Range Weather Forecasts (Table 1), primarily due to the overestimation of the ERA5 precipitation estimate. Sun and Su (2020) indicated that the contribution of glacier runoff would increase by 7–10% with a unit decrease in mean annual precipitation. Therefore, an accurate precipitation estimate is crucial as a model input to simulate runoff regimes, and further quantify the effect of glaciers and snowmelt on runoff in the NX basin.

These uncertainties in the hydrological simulation will be introduced and enlarged on the uncertainty in future projections (Lutz et al. 2016). Existing studies of hydrological responses to future climate changes have been a debate in the NX sub-basin of the YZ basin. For

https://doi.org/10.5194/hess-2024-11
Preprint. Discussion started: 23 January 2024


Hydrology and Earth System Sciences
Discussions

example, Lutz et al. (2014) forced the Spatial Processes in Hydrology (SPHY) model using outputs from 4 global climate models (GCMs) and showed that runoff would be increased by 3–13% relative to the reference period 1998–2007 until at least 2050s due to the increasing precipitation in the YZ basin. Zhao et al. (2019) projected the future runoff changes with 5 GCM outputs using an extended Variable Infiltration Capacity (VIC) macroscale hydrological model (VIC-CAS), suggesting that the total runoff will increase by 16–31% by the end of this century relative to the reference period 1970–2010 because of increased rainfall-induced runoff in the YZ basin. Cui et al. (2023) also suggested that total runoff in the YZ basin will increase of 7.3±11% by 2070s relative to the 1985–2014 resulted from rainfall runoff. Meanwhile, Su et al. (2016) projected a runoff increase of 6.7–14.4% in the 2041–2070 relative to the reference period 1971–2000 in the YZ forced by the VIC-Glacier model with ensemble outputs of 20 GCMs, and attributed the runoff increases to the rising glacier melt runoff. In addition, future flow evolution and the effect of different runoff compositions on total runoff in the NX-BXK are also unclear.

To address these issues, this study divided the YZ into six sub-basins and collected streamflow observations at three hydrological stations (Yigong, Bomi, and Motuo) and glacier mass balance observations (Parlung No.94) in the NX-BXK sub-basin, filling in the gap of scarce data coverage. Additionally, streamflow observations at five national hydrological stations and glacier mass balance observations at a site (Gurenhekou) in the five sub-basins of

https://doi.org/10.5194/hess-2024-11
Preprint. Discussion started: 23 January 2024


Hydrology and Earth System Sciences
Discussions

the NX (Figure 1), together with hydrological stations in the NX-BXK, constitute a unique observation basis. This basis allows us to validate the glacier-hydrology model and reveal runoff regimes, and changes at the sub-basin scale. Precipitation observations at 280 gauges, were collected, and a high spatiotemporal resolution (10 km; daily) precipitation dataset was generated using a machine learning algorithm based on these gauges (Sun et al., 2022).

Leveraging this basin-wide observation dataset, this study comprehensively investigates runoff compositions, changes, and attributions across six sub-basins in the YZ for 1971–2020, with a particular focus on the comparison between the NX and NX-BXK. This investigation employs the process-based and well-established Variable Infiltration Capacity (VIC)-Glacier hydrological model. Furthermore, the study assesses the future evolution of annual and seasonal total water availability, glacier runoff, and snowmelt, using an ensemble of multiple global climate models (GCMs) from the latest release of the Coupled Model Intercomparison Project Phase 6 (CMIP6). The objectives are to: (1) use the model framework to identify spatiotemporal characteristics in runoff compositions and changes at the sub-basin scale under heterogeneous climate and glacier/snow conditions. (2) quantify the contributions of three major runoff compositions (glacier, rainfall, and snowmelt runoff) to total runoff among different sub-basins, and investigate their responses to climate changes. (3) assess future water availability under 21st-century climate-cryosphere change, assisting policy-makers and water managers in adopting strategies. These findings are anticipated to provide a basic

https://doi.org/10.5194/hess-2024-11
Preprint. Discussion started: 23 January 2024


Hydrology and Earth System Sciences
Discussions

framework for studying cryospheric basin hydrological cycles in the TP and provide adaptation strategies for rational water resource management, and social, and economic development grounded in a robust scientific understanding.

2 Study Area

In this study, the YZ basin is divided into six sub-basins based on flow direction and locations of hydrological stations (Figure 1; Table 2). There are five sub-basins located upstream of the Nuxia (NX) hydrological station, collectively termed the NX basin, with an additional sub-basin lying between Nuxia and Pasighat (NX-BXK) hydrological stations. The NX basin comprises the upstream sub-basins of Lhatse (LZ), Shigatse (RKZ), and Lhasa (LS) hydrological stations, along with the sub-basins between Lhatse and Yangcun (LZ-YC) hydrological station and between Yangcun and Nuxia (YC-NX) hydrological station.

The climate in the YZ is characterized by a wet and warm summer and a cool, dry winter, with precipitation mostly dominated by the summer monsoon, contributing 70–90% of annual totals during June–September (Figure S1). Furthermore, mean annual precipitation increases downstream in the YZ basin, ranging from 283 mm upstream to 1465 mm downstream, averaging about 774 mm for the entire YZ basin (Table 2). All sub-basins exhibit similar seasonal temperature patterns, with peaks mainly occurring in July–August (Figure S1). Glacier coverage varies from 0.9% (LZ-YC) to 10.2% (NX-BXK), averaging 3.3% for the

https://doi.org/10.5194/hess-2024-11
Preprint. Discussion started: 23 January 2024


Hydrology and Earth System Sciences
Discussions

entire YZ basin. The YC-NX (2.8%) and NX-BXK (10.2%) sub-basins host the most extensive glacier coverage (Table 1). The mean annual snow cover fraction (SCF) ranges from 7% (RKZ) to 32% (NX-BXK), with an average of 19% across the YZ basin.

3 Data and Method

3.1 Data

Daily precipitation, maximum and minimum temperature, and wind speed estimates with a spatial resolution of 10×10 km were used as the VIC-Glacier model forcing inputs in this work. Historical meteorological data during 1971–2100 was adopted from Sun et al. (2022), which corrected these data by machine learning algorithm based on estimates form meteorological stations and the ERA5. The daily gridded precipitation estimates from the ERA5 was corrected based on 580 rain gauges in the monsoon-dominated TP region (290 rain gauges in the YZ basin, Figure 1), and was inversely evaluated by the VIC-Glacier model, suggesting the good potential utility in model simulation in the YZ basin (Sun et al., 2022). It was downloaded from the National Tibetan Plateau/Third Pole Environment Data Center (TPDC, https://doi.org/10.11888/Atmos.tpdc.272885).

Using the newly generated daily meteorological data for 1961–2020, Sun et al. (2024) applied the Bias Corrected Spatial Disaggregation (BCSD) statistical downscaling approach (Wood 2002; Wood et al. 2004) to downscale and bias-correct daily transient meteorological data,

https://doi.org/10.5194/hess-2024-11
Preprint. Discussion started: 23 January 2024

including precipitation, maximum and minimum temperature, and wind speed, with a spatial resolution of 10×10 km through the 21st century from 10 GCMs from the CMIP6 under the Shared Socioeconomic Pathways (SSPs)2-4.5 and SSP5-8.5 scenario. Daily transient climate estimates, at a spatial resolution of 10×10 km for 1971–2100 under 20 scenarios (10 GCMs × 2 SSPs) from Sun et al. (2024) were directly employed to drive the VIC-Glacier model to continuous runoff production in the YZ basin.

Observed streamflow, observed glacier mass balance, satellite-based glacier area and snow cover fraction estimates were applied to calibrate and validate the model in this study. Monthly streamflow since 1971 were collected at eight hydrological stations (Lhatse, Shigatse, Lhasa, Yangcun, Nuxia, Yigong, Bomi, and Motuo from the Ministry of Water Resources, China (Figure 1, Table S1).

Two shapefiles of glacier inventory, the first Glacier Inventory of China (CGI) from the "Environment & Ecological Science Data Center for west China" (http://westdc.westgis.ac.cn/glacier) and Randolph Glacier Inventory (RGI) 6.0 (https://www.glims.org/RGI/rgi60_dl.html), were used to describe the glacier information of the YZ in the VIC-Glacier model. Observed annual glacier mass balance data from Gurenhekou and Parlung No.94 glacier sites since 2005 were used to validate the performance of glacier model (http://www.tpdc.ac.cn, Figure 1, Table S1). The Moderate Resolution

https://doi.org/10.5194/hess-2024-11
Preprint. Discussion started: 23 January 2024


Hydrology and Earth System Sciences
Discussions

Imaging Spectroradiometer (MODIS) 10CM reporting the maximum percentage of snow cover during an 8-day period in 0.05° resolution grid (https://nsidc.org/ data) during 2006–2018 was used to calculate the snow cover fraction (SCF) and to compare with VIC-Glacier model simulations in the YZ basin.

The model required land surface characteristics, including soil texture and vegetation types, were adopted from Sun and Su (2020). These data were used as initial model inputs, and remained unchanged in simulation period.

3.2 VIC-Glacier Hydrological Model

The present study employed the physically-based and distributed VIC hydrological model (Liang et al., 1994; Liang et al., 1996) linked with a simple degree-day glacier melt algorithm (Hock, 2003), referred to as VIC-Glacier. This modeling framework facilitates the comprehensive simulation of the physical exchange of water and energy within a grid mesh encompassing soil, vegetation, and the atmosphere. The VIC-Glacier effectively models surface water balance compositions, including evapotranspiration, surface runoff, baseflow (subsurface drainage into the local stream channel network, as opposed to groundwater recharge), and total soil moisture, including liquid and ice content in each soil layer. The model integrates a two-layer energy-balance snow model (Cherkauer and Lettenmaier, 1999) and a frozen soil/permafrost algorithm (Cherkauer and Lettenmaier, 1999; 2003). These

https://doi.org/10.5194/hess-2024-11
Preprint. Discussion started: 23 January 2024


Hydrology and Earth System Sciences
Discussions

components account for ground snowpack, snow within the vegetation canopy, snow atop lake ice, and sublimation of snow. In each time step, the model calculates the rain or snow fraction contributing to the snowpack. Subsequently, all energy fluxes are computed, triggering melt if the energy balance is positive. The VIC-Glacier model has demonstrated its effectiveness in hydrological simulations for various high-mountainous TP basins (Meng et al., 2019; Su et al., 2016; Sun and Su, 2020; Tong et al., 2016; Zhang et al., 2013; Zhao et al., 2019).

Here, the modeling framework at a 10 km ×10 km spatial resolution and a three-hourly time step was adopted from Sun and Su (2020). To categorize the total runoff sources in this study, we partitioned it into three components: rainfall runoff, snowmelt runoff, and glacier runoff. Glacier runoff was defined as all water generated in the glacierized area, including rainfall, snow melt, and ice melt in the glacierized area. Recognizing the influence of glacier melt at different elevations, each glacierized grid cell underwent division into various elevation bands with an interval of 100 m (Kan et al., 2018). The simulated total runoff of each grid is from both the glacierized and non-glacierized areas, that is,

$$R_i = f \times R_{glac} + (1 - f) \times R_{vic} \quad (1)$$

Where, R_i is the total runoff (mm) in grid *I*, *f* is the percentage of glacier area, and glacier area is updated every year, R_{glac} is the runoff (mm) from the glacier area calculated by the glacier model, and R_{vic} is the sum of surface runoff and baseflow runoff (mm) for non-glacierized

https://doi.org/10.5194/hess-2024-11
Preprint. Discussion started: 23 January 2024


Hydrology and Earth System Sciences
Discussions

areas calculated by the VIC model, including both rainfall and seasonal snowmelt runoff. R_{glac} can be calculated as:

$$M_i = \begin{cases} DDF \times (T - T_{base}); T > T_{base} \\ 0; \qquad\qquad\quad T \leq T_{base} \end{cases} \qquad (2)$$

$$R_{glac} = M_1 + M_2 + \cdots + M_i; i = 1, 2, 3, \ldots, n \qquad (3)$$

where, M_i is the meltwater (mm) from elevation band *j* and *n* is the total number of elevation bands in grid *i*; *DDF* is the degree-day factors of glacier or snow melt (mm °C^{-1} day^{-1}); *T (°C)* is the daily average air temperature above the glacier surface; T_{base} (°C) is the temperature threshold for glacier and snow melt (0 °C). In a precipitation event, rainfall occurs when the air temperature is above 0°C; otherwise, it snows. In the presence of a snowpack on the glacier, the snow melts first before glacier melting starts, following the same degree-day approach but different degree-day factors.

The calculated glacier area and volume were updated every year in the model by the volume-area scaling approach (Bahr et al., 1997). An exponential form (equation 2), derived from glacier observations in western China (Liu et al., 2003), converts glacier area to volume for a basin:

$$V = 0.04S^{1.35} \qquad (4)$$

Where, *V* is glacier volume and *S* is glacier area. Initial glacier volume was determined using glacier area data from the first Glacier Inventory of China (CGI V1.0, http://westdc.westgis.ac.cn/glacier) dataset, which presented glacier area for period 1970s−1990s. The Randolph Glacier Inventory (RGI V6.0) dataset presented glacier area for period 2000s−2010s. Therefore, glacier area was simulated by glacier model since 1971, and

https://doi.org/10.5194/hess-2024-11
Preprint. Discussion started: 23 January 2024


Hydrology and Earth System Sciences
Discussions

304 then it was updated every year with the snowfall accumulation and simulated ice melt from all
305 the glacier cells in the glacier model based on volume-area scaling approach. The simulated
306 mean annual glacier area during 2000−2010 was compared with the Randolph Glacier
307 Inventory (RGI V6.0) dataset in the YZ basin and its six sub-basins.

308

309 **3.3 Model Calibration and Validation**

310 The VIC-Glacier model requires the calibration of two sets of parameters: (1) the degree day
311 factor (DDF), related to glacier runoff simulation; and (2) VIC model parameters related to
312 runoff simulation in non-glacierized regions. The latter includes parameters such as the depth
313 of the first and second soil layers (D1 and D2), the infiltration shape parameter (B_inf), and
314 three base flow parameters, including the maximum velocity of baseflow (Dsmax), a fraction
315 of Dsmax where non-linear baseflow begins (Ds), and a fraction of maximum soil moisture
316 where non-linear baseflow occurs (Ws).

317

318 To adjust the internal stores of energy and water from the initial state to equilibrium, the VIC-
319 Glacier model underwent a spin-up from 1961–1970, with subsequent simulation for the years
320 1971–2020. In addition, 1971–2000 was selected as the calibration period and 2001–2015 the
321 validation period based on the observed monthly streamflow for 1971–2015. Calibration and
322 validation of the VIC-Glacier hydrological model followed a systematic two-step approach,
323 employing observed streamflow, glacier mass balance, and satellite-based estimates of glacier

https://doi.org/10.5194/hess-2024-11
Preprint. Discussion started: 23 January 2024


Hydrology and Earth System Sciences
Discussions

area and snow cover fraction (Table S1). Model performance was assessed using metrics such as Nash-Sutcliffe efficiency (NSE), relative bias (RB, %), and correlation coefficient (CC). The optimization process utilized a trial-and-error method to minimize bias against predefined criteria. Linear regression was employed to calculate annual and seasonal trends of precipitation, temperature, and runoff.

The model calibration and validation were conducted using a two-step approach to overcome equifinality problems. First, initial values of DDF parametersin the glacier model related to glacier and snowmelt were adopted from Sun and Su (2020). The glacier model was calibrated to match the glacier area observations from RGI V6 for 2000s−2010s in the YZ and six sub-basins, and validated by observed mass balance data from the Gurenhekou site in the NX basin and the Parlung No.94 glacier site in the NX-BXK sub-basin (Figure S2). Given the good performance in simulating glacier area (with RB of mostly < 7%, Figure 2c) and good consistency (CCs of 0.65–0.96) in annual variations between observed glacier mass balance and simulation, final DDF values (6.5–11.0 $mm°C^{-1}$ day^{-1}) were determined across six sub-basins (Table 3).

Second, the VIC-related parameters were validated against observed streamflow and satellite-based snow cover fraction (SCF) data. The infiltration parameter (B_inf) and the second soil layer depth (D2) have been identified as the most sensitive parameters (Zhang et al., 2013).

https://doi.org/10.5194/hess-2024-11
Preprint. Discussion started: 23 January 2024


Hydrology and Earth System Sciences
Discussions

The B_inf which defines the shape of the variable infiltration capacity curve has a common range of 0–0.4, while the D2 mainly determines the moisture storage capacity of the VIC model, with a range of 0.5–1.0 (Liang et al., 1996; Shi et al., 2008). The simulated monthly streamflow captured well the magnitudes and patterns of observation at eight hydrological stations, with NSEs of 0.71 to 0.86 and RBs of within ±8% for the calibration and validation period across the sub-basins (Table 3, Figure S3). To further validate the model, monthly satellite-based SCF data for the years 2001–2019 in the YZ basin were compared with the model simulations (Figure S4). The simulated SCF closely mirrors the monthly variations observed in the satellite-based data, exhibiting a CC of 0.60–0.82 ($p < 0.05$) and RB within ±12% across sub-basins. This alignment suggests the VIC-Glacier model's satisfactory performance in simulating snow cover dynamics in the YZ basin.

4 Result

4.1 Hydrological Response to Historical Climate Changes

4.1.1 Runoff Composition

The credibility of our model allows for a reasonable interpretation of the current runoff composition and change, and their responses to climate change. Examining simulated streamflow across sub-basins reveals significant differences in each sub-basin contribution to the total runoff at the Pasighat outlet of the YZ basin (Figure 1b). The NX-BXK emerges as the most critical runoff-generating area, contributing approximately 52% to the total runoff in the YZ basin, followed by YC-NX (25%), LS (10%), and other sub-basins with contributions

https://doi.org/10.5194/hess-2024-11
Preprint. Discussion started: 23 January 2024


Hydrology and Earth System Sciences
Discussions

365 ranging from 3% to 6%.

366

367 According to the source of runoff generation, total runoff is partitioned into three
368 compositions in this study: rainfall runoff, snowmelt runoff, and glacier runoff. In this study,
369 glacier runoff is defined as all water generated in the glacierized area, including rainfall, snow
370 melt, and ice melt in the glacierized area. Rainfall and snowmelt runoff are originating from
371 the non-glacierized area. Different runoff regimes of rainfall runoff, snowmelt, and glacier
372 runoff influence their contributions to total runoff across the six sub-basins of the YZ with
373 heterogeneous surface characteristics (Figure 2). Rainfall runoff dominates the mean annual
374 total runoff in the YZ and all its sub-basins from 1971 to 2020, contributing 59%–78% to
375 annual total runoff, with an average of 62% in the entire YZ basin. Snowmelt contributes 22%
376 to annual total runoff in the YZ basin, varying from 14% to 36% across six sub-basins, with
377 the LS sub-basin having the largest contribution at 36%. Glacier runoff contributes 16% to the
378 annual total runoff in the YZ basin, ranging from 5% to 19% across six sub-basins for 1971–
379 2020. The highest contributions are in the NX-BXK (19%) and YC-NX (16%) sub-basins,
380 which have the largest glacier coverage in the YZ basin (Table 2).

381

382 Figure 3 shows the spatial pattern of average annual rainfall runoff, snowmelt, and glacier
383 runoff for 1971–2020, along with their percentages at different elevation bands in the YZ
384 basin. The spatial pattern of average annual rainfall runoff (Figure 3a) is similar to that of

https://doi.org/10.5194/hess-2024-11
Preprint. Discussion started: 23 January 2024


Hydrology and Earth System Sciences
Discussions

385 total runoff (Figure 1b) and precipitation (Figure 3b), decreasing from east to west, with the
386 NX-BXK sub-basin exhibiting the largest runoff. Similarly, the largest snowmelt and glacier
387 runoff occur in the NX-BXK sub-basin, consistent with the spatial distribution of glacier and
388 snow cover area, constituting about 65% of total glacier area and 34% of total snow coverage
389 in the YZ (Figure 3c–f). Approximately 84% of the YZ basin runoff originates from middle
390 altitudes (3500–5500 m), with 62% from 4500–5500 m and 22% from above 3500–4500 m,
391 primarily contributed by rainfall and seasonal snow (80%–83%, Figure 3g). About 8% of the
392 basin runoff is generated from high altitudes (>5500 m), where 29% of the flow is from
393 glacier runoff, and the remainder is from rainfall (50%) and snowmelt (21%). In low altitudes
394 (<3500 m), 8% of the basin runoff is primarily from rainfall (82%) and snowmelt (11%), with
395 only 7% attributed to glacier runoff.
396
397 The seasonal pattern of total runoff remains consistent across the six sub-basins within the YZ
398 for 1971–2020, with more than 60% of the annual total runoff occurring in June–September
399 and 10%–15% in November–February (Figure 2a–h). This seasonal pattern aligns with the
400 rainfall runoff, which peaks in July–August, reflecting the peak in total runoff in the YZ and
401 its sub-basins (Figure 2 a–h). Snowmelt predominantly takes place from April–October, with
402 peak months varying across sub-basins. In LZ, RKZ, LS, and LZ-YC sub-basins, the peak is
403 in July–September (Figure 2a–d), attributed to the melting of fresh snowfall in the warm
404 season. Conversely, in the YC-NX (Figure 2e) and NX-BXK (Figure 2f) sub-basins, the peak

https://doi.org/10.5194/hess-2024-11
Preprint. Discussion started: 23 January 2024


Hydrology and Earth System Sciences
Discussions

is in May–June, possibly due to snowfall accumulation during October–March. Simulated glacier runoff occurs mainly from June to September for all basins, peaking in July–August, coinciding with the co-occurrences of peak precipitation and temperature.

4.1.2 Runoff Changes and the Response to Climate Changes

(a) Annual Scales

Figure 4 illustrates annual trends in precipitation, temperature, total runoff, and three runoff compositions (rainfall, glacier, and snowmelt runoff) across the six sub-basins for 1971–2020, respectively. Annual variations for precipitation, temperature, and simulated runoff in each sub-basin are presented in Figure S5–S10. All sub-basins exhibit significant warming trends (0.3–0.5 °C/10yr, $p<0.05$), with precipitation tending to increase (6–15 mm/10yr) in the LZ, LZ-YC, LS, RKZ, and YC-NX sub-basins (Figure 4a–e) upstream of the NX hydrological station (NX basin). Conversely, the NX-BXK sub-basin experiences a significant decrease in precipitation (-35 mm/10yr, $p<0.05$, Figure 4f).

Simulated annual total runoff demonstrates increasing trends of 8.1–18.8 mm/10yr for 1971–2020 across all sub-basins within the NX basin, except for the RKZ sub-basin with an insignificant change (-1.1 mm/10yr), resulting in a significantly increasing trend of 9.4 mm/10yr ($p<0.05$) over the entire NX basin (Table 4). Strong correlations between annual variation of total runoff, precipitation, and rainfall runoff exist in these sub-basins (CC of

https://doi.org/10.5194/hess-2024-11
Preprint. Discussion started: 23 January 2024


Hydrology and Earth System Sciences
Discussions

425 0.90–0.99, p<0.05), while total runoff shows weak relationships with temperature and glacier
426 runoff. This suggests the predominant role of rainfall runoff from nonglacierized areas, with
427 minor impacts from glacier runoff on annual runoff, along with significant increases in
428 precipitation and temperature (Figure 4a). In contrast, the NX-BXK sub-basin exhibits a
429 significantly decreasing trend of 9.4 mm/10yr (p<0.05) for 1971–2020 (Figure 4f), resulting
430 from significant decreases in rainfall runoff (-22 mm/10yr) and seasonal snowmelt (-5.5
431 mm/10yr) from non-glacierized areas. Glacier runoff, however, exhibits a significantly
432 increasing trend (6.0 mm/10yr, p<0.05, Table 3) in NX-BXK during the same period, partially
433 compensating for the decreasing trend of total runoff in this sub-basin. The integrated result is
434 a weakly increasing trend of 3.1 mm/10yr in total runoff for the entire YZ basin (Table 4),
435 primarily attributed to increases in rainfall (3.0 mm/10yr) and glacier runoff (2.1 mm/10yr).
436 Snowmelt tends to decrease (-1 to -6 mm/10yr) in the YZ and its sub-basins during 1971–
437 2020, associated with a reduction in solid precipitation and an increase in liquid precipitation
438 (Figure S12), along with significant temperature increases.
439
440 Cuo et al. (2019) investigated precipitation and streamflow mutations in the YZ basin using
441 Mann-Kendall analysis, identifying a streamflow mutation in 1997 at the NX hydrological
442 station. This abrupt change is consistent with our long-term runoff observations. This abrupt
443 change is consistent with our long-term runoff observations. Total runoff trends are opposite
444 before and after the year 1998 in the YZ, and its NX and NX-BXK sub-basins (Table 4).

https://doi.org/10.5194/hess-2024-11
Preprint. Discussion started: 23 January 2024


Hydrology and Earth System Sciences
Discussions

During 1971–1997, annual total runoff shows increasing trends (8.9–48.1 mm/10yr) in the basins during 1971–1997, mainly due to an increasing trend in rainfall and glacier runoff (Table 4). However, during 1998–2020, total runoff showed insignificant decreasing trends (-0.3 to -3.3 mm/10yr), attributed to a decreasing trend in rain runoff induced by the weakening Indian monsoon from 1998–2000 (Table 4). It is noteworthy that the rate of decrease in precipitation is faster in NX-BXK (-16.0 mm/10yr) than in NX (-7.0 mm/10yr, Table 4). However, the decline in total runoff is less pronounced in NX-BXK (-0.3 mm/10yr) compared to NX (-3.3 mm/10yr, Table 3) during 1998–2000. This discrepancy arises from different influences of glacier runoff on total runoff between NX and NX-BXK sub-basins. A more rapid increase in glacier runoff in NX-BXK (16 mm/10yr) than in NX (0.7 mm/10yr, Table 4) partly compensates for the quicker decline in rainfall-runoff, resulting in a slower overall decrease in total runoff in NX-BXK.

Figure 5 illustrates the mean monthly vertical integral of atmospheric moisture budget in June, July, August, and September from ERA5 data across the YZ basin for 1971–2020. It demonstrates an increasing trend in the NX basin but a decreasing trend in the NX-BXK. This pattern corresponds with precipitation trends in the NX and NX-BXK sub-basins, influencing rainfall runoff in these areas. Additionally, teleconnection indices can modulate circulation patterns over a region, thereby affecting precipitation and its induced runoff. Among the 10 teleconnection indices (Text S1), Pacific Decadal Oscillation (PDO) and El Niño/Southern

https://doi.org/10.5194/hess-2024-11
Preprint. Discussion started: 23 January 2024


Hydrology and Earth System Sciences
Discussions

Oscillation (ENSO) exhibit significantly negative consistency with precipitation, while Atlantic Multidecadal Oscillation (AMO) shows significantly positive consistency (CC=0.43, $p<0.05$) with precipitation for 1971–2020 in the NX basin (Figure S13a, d). The change in runoff induced by precipitation is mostly influenced by EASM with significantly positive consistency (CC=0.38, $p<0.05$) for 1971–2020 in the NX-BXK sub-basin (Figure S13a, e). The streamflow mutation in 1997, associated with the precipitation mutation, is also influenced by NAO and ENSO in the NX and EASM in the NX-BXK.

(b) Seasonal Scales

Because of the similarity in annual runoff regimes and changes across five sub-basins within the NX basin, here, we particularly focus on comparing the NX and NX-BXK sub-basins at seasonal scales for 1971–2020. The high-altitude NX basin exhibits faster warming trends (0.2–0.5 °C/10yr) in each season compared to the low-altitude NX-BXK basin (0.16–0.23 °C/10yr, Figure 6d) for 1971–2020. Seasonal precipitation trends increase (2–9 mm/10yr) for 1971–2020 in the NX basin (Figure 6a), particularly in summer, influenced mainly by the AMO and PDO (Figure S14). Conversely, in the NX-BXK, precipitation decreased (-18 to -2 mm/10yr) for 1971–2020, influenced by the EASM in summer and the AMO in autumn. Consequently, total runoff during 1971–2020 reflects similar trends to precipitation, affected by increased rainfall (1–6 mm/10yr) and glacier runoff (1 mm/10yr) in the NX (Figure 6a), and decreased rainfall (-10 to -3 mm/10yr) and snowmelt (-2 mm/10yr), along with increased

https://doi.org/10.5194/hess-2024-11
Preprint. Discussion started: 23 January 2024


Hydrology and Earth System Sciences
Discussions

485 glacier runoff (1–5 mm/10yr) in the NX-BXK (Figure 6b). Due to these different trends in the
486 two sub-basins, total runoff shows an increasing trend in summer (5 mm/10yr) but decreasing
487 trends (-1 mm/10yr) in other seasons for 1971–2020 in the YZ basin (Figure 6c), attributed to
488 the dominance of rainfall runoff.
489
490 Relative to the period 1971–1997, divergent seasonal changes in total runoff are apparent in
491 the YZ basin during 1998–2020 (Figure 7). In the NX basin, total runoff tends to increase by
492 about 5%–22% in all seasons, with the largest increases during May–August (11%–22%),
493 mainly due to increases in rain-induced and glacier runoff. The smallest increases occur
494 during December–February (5%–6%), mostly due to increased rainfall runoff (3%–5%) in the
495 NX (Figure 7a, d; Table S2). Snowmelt significantly increases during March–May (24%–50%)
496 due to early snow melting (Figure 7d; Table S2), potentially benefiting agricultural water
497 supplies. Conversely, total runoff in the NX-BXK sub-basin decreases by about 3%–20% in
498 all seasons (Figure 7b; Table S2) due to declines in rainfall runoff (3%–23%) and seasonal
499 snowmelt (4%–28%). This indicates a trend toward drier conditions, although increased
500 glacier runoff (2%–12%) somewhat compensates for the loss of total runoff in July–August
501 (Figure 7e). The integrated result of seasonal runoff changes in NX and NX-BXK shows total
502 runoff in the YZ increases by 2%–4% in June–September, mostly due to increases in rain-
503 induced (3%–7%) and glacier runoff (2%–6%), while it decreases in other months due to
504 decreased rain-induced runoff (2%–8%) and seasonal snowmelt (3%–10%, Figure 7c, f, Table

https://doi.org/10.5194/hess-2024-11
Preprint. Discussion started: 23 January 2024


Hydrology and Earth System Sciences
Discussions

505 S2).

506

507 The distinct seasonal changes in rainfall, snowmelt, and glacier runoff largely play a crucial
508 role in determining the seasonal shifts in their contributions to total runoff across the entire
509 YZ basin and its NX and NX-BXK sub-basins. Compared to the period 1971–1997, the
510 contribution of rainfall increases by 5%–8% from May to October in the NX for 1998–2020,
511 whereas glacier and snowmelt contributions decline by -0.3% to -2% and -5% to -7%,
512 respectively (Figure 7g, Table S2). Conversely, in the NX-BXK, contributions from rainfall
513 runoff and snowmelt decrease by -2% to -6% during May–October, while glacier contribution
514 increases by 2%–7% in these months (Figure 7h, Table S2), underscoring the growing
515 significance of this season in sustaining summer water supplies in the NX-BXK. Taken
516 together, for the entire YZ basin (Figure 7i), glacier contribution increases by 0.5%–2%
517 (Table S2) during June–October, and the seasonal changes in rainfall and snowmelt
518 contributions to total runoff closely mirror those observed in the NX basin.

519

520 **4.2 Hydrological Response to Future Climate Changes**

521 Historical differences in total runoff changes in the NX and NX-BXK sub-basins are
522 projected to weaken in the future. The YZ basin is projected to experience increased
523 precipitation (7–33 mm/10yr) and higher temperatures (0.3–0.8 °C/10yr) under the SSP2-4.5
524 and SSP5-8.5 scenarios throughout the 21st century (Table 5). Predictions indicate an increase

https://doi.org/10.5194/hess-2024-11
Preprint. Discussion started: 23 January 2024


Hydrology and Earth System Sciences
Discussions

525 in total runoff for the NX (7–27 mm/10yr) and BXK (34–100 mm/10yr) for 2021–2100 under
526 both SSPs, with significant increases (36–142 mm/10yr) anticipated in the latter half of the
527 century (2071–2100) under SSP5-8.5 (Table 5). The changes in total runoff are projected to be
528 primarily influenced by increased rainfall runoff, with minor contributions from increased
529 snowmelt and glacier runoff under both SSPs scenario through the 21st century (Table 5).
530 However, in comparison to the 1971–2000 mean, a reduction of approximately -6% to -14%
531 is projected in the first half of the 21st century (2021–2050) in the YZ and its NX and NX-
532 BXK sub-basins under the SSP2-4.5 and SSP5-8.5 scenario (Figure 8). This reduction is
533 attributed to decreased rainfall (-9% to -19%) and snowmelt (-5% to -6%), which may result
534 in the decline of freshwater supply. Conversely, there is a broadly consistent increase (6%–
535 32%) in total runoff in the second half of the 21st century (2071–2100), mainly driven by
536 increased rainfall (4%–52%) and glacier runoff (9%–78%), suggesting that the YZ basin will
537 not face a water supply crisis in the end of 21st century.
538
539 Changes in meltwater from glaciers and seasonal snow significantly impact total runoff,
540 influencing both quantity and timing and are particularly important for water availability
541 during warm and dry seasons (Barnett et al., 2005). Relative to the 1971–2000 mean, the
542 future annual hydrograph appears relatively stable across all sub-basins (Figure 9), with 60%–
543 80% of mean annual runoff occurring from June to September. However, a decline of about -
544 18% to -3% is projected in each month during 2021–2050 under the two SSPs due to

https://doi.org/10.5194/hess-2024-11
Preprint. Discussion started: 23 January 2024


Hydrology and Earth System Sciences
Discussions

545 decreased monthly precipitation and precipitation-induced rainfall and snowmelt runoff
546 (Table S3 and S4). In contrast, there is an anticipated increase of about 6%–40% in each
547 month, particularly in summer (25%–40%), during 2071–2100 under the two SSPs. The
548 increased total runoff in the NX basin is primarily attributed to increased rainfall runoff and
549 spring snowmelt, indicating an earlier spring snow melt and delayed fall freeze-up (Figure 9a,
550 b). Similarly, the increased total runoff in the NX-BXK basin is mostly a result of increased
551 rainfall and glacier runoff, coupled with decreased snowmelt (Figure 9c, d), primarily due to
552 reduced snowfall with ongoing warming in each month (Figure S4 and S5). Future changes in
553 seasonal runoff across the entire YZ basin closely align with those in the NX-BXK sub-basin
554 (Figure 9e, f) due to its significant contribution to the overall runoff of the YZ basin.
555
556 **5 Discussion**
557 **5.1 Uncertainty**
558 Forcing inputs, parameters, and representation of physical processes are major sources of
559 uncertainty in hydrological model simulations.
560
561 Precipitation is the most important atmospheric input for land surface hydrology models, but
562 none of the multiple precipitation datasets proves equally suitable for all basins in the TP due
563 to the high spatiotemporal variability in their performance at the sub-basin scale (Dahri et al.
564 2021). The variation in precipitation datasets for high mountains can lead to significant

https://doi.org/10.5194/hess-2024-11
Preprint. Discussion started: 23 January 2024


Hydrology and Earth System Sciences
Discussions

565 differences in meltwater contribution (Lutz et al., 2014; Zhao et al., 2019; Sun and Su, 2020;
566 Khanal et al., 2021; Nan et al., 2021; Wang et al., 2021). Duethmann et al. (2014) applied a
567 multi-objective genetic algorithm to characterize the trade-off curve between model
568 performance in terms of discharge and snow cover area in Central Asia, suggesting that good
569 discharge simulations at the catchment outlet cannot guarantee good internal functioning of
570 the model, as different forcing inputs may result in error compensation among different runoff
571 compositions. Jost et al. (2012) simulated glacier runoff of 25 large glacierized basins
572 (>50,000 km^2) in North and South America, Europe, Asia, and New Zealand, suggesting that
573 the runoff differences ranged from 0.07 % for weakly glacier-influenced basins to 252 % for
574 strongly glacier-influenced basins. They also suggested that hydrologic model calibration in
575 glacier-fed catchments was difficult, because errors in modelling snow accumulation can be
576 offset by compensating errors in glacier melt. Zhang et al. (2013) simulated glacier runoff by
577 the VIC-Glacier model with the APHRODITE precipitation estimates in the upper Indus (UI)
578 river basin of the TP during 1961–2009, and suggeted that contribution of glacier runoff to
579 total runoff was about 48.2. However, Meng et al. (2023) simulated glacier runoff by the
580 VIC-Glacier model with the corrected MERRA-2 precipitation estimates in the UI basin,
581 suggested that glacier runoff contributed of 24% to total runoff. The difference between
582 Zhang et al. (2013) and Mengand (2023) mostly resulted from the higher amount of corrected
583 MERRA-2 than APHRODITE precipitation estimates in the UI basin, because the
584 underestimation of precipitation-induced runoff would be compensated by glacier runoff.

https://doi.org/10.5194/hess-2024-11
Preprint. Discussion started: 23 January 2024


Hydrology and Earth System Sciences
Discussions

585

586 Like elsewhere on earth, the aforementioned issues are typical of the YZ basin. In the case of
587 the NX basin, glacier melt contributed approximately 2–18% to the total runoff in existing
588 research (Table 1), mostly resulting from differences in forcing inputs used in hydrological
589 models. The YZ basin received less attention regarding glacier runoff contributions in the
590 NX-BXK, with significant inconsistencies in glacier contributions evident in these studies
591 (Table 1). Sun and Su (2020) suggested that mean annual glacier runoff contributed about 45%
592 to total runoff in the NX-BXK sub-basin for 1980–2000, using a hydrological model without
593 calibration and validation due to a lack of hydrometeorological observations in the sub-basin.
594 In this study, we utilized newly acquired rain gauge data, and streamflow, glacier mass
595 balance, and glacier and snow cover observations in the NX-BXK sub-basin, glacier runoff
596 was simulated using the well-validated VIC-Glacier model, forced by a comprehensively
597 reconstructed long-term precipitation dataset in this study. The updated contribution of glacier
598 runoff to total runoff during 1971–2020 in the NX-BXK sub-basin was determined to be 19%.
599 Furthermore, accurate historical precipitation estimates have the potential to reduce
600 uncertainty in future projections with the large spread in the GCMs, forming the basis for
601 correcting future GCM estimates. Different study period also results in the difference of
602 hydrological model simulation. For example, streamflow also mutates in 1997 at the RKZ
603 sub-basin of the YZ (Figure S15). Increased precipitation and evaporation caused an
604 insignificant runoff change during 1971–1997. However, due to significant decrease of

https://doi.org/10.5194/hess-2024-11
Preprint. Discussion started: 23 January 2024


Hydrology and Earth System Sciences
Discussions

605 precipitation and increase of evaporation, runoff decreased during 1998–2000, resulting in the
606 insignificant decrease for 1971–2000 (Figure S15).
607
608 Hydrological model themselves have their own uncertainties, such as model parameters and
609 structure of physical processes, which are ideally all taken into account. Reliable parameters
610 play a crucial role in accurate runoff simulation by hydrological models. The DDF emerges as
611 the most sensitive parameter for the degree-day glacier model (Hock 2003; Radić; Hock
612 2010). Zhang et al. (2013) examined the sensitivity of glacier melt runoff to DDF parameters,
613 suggesting that average annual glacier runoff could change by about 10% with each one unit
614 change in DDF (mm $°C^{-1}$ day^{-1}). In this study, the DDF parameters are derived based on
615 observed glacier mass balance data, with intensive validations on glacier melt, including
616 observed glacier mass balance and satellite-based glacier area estimates. The uncertainty
617 associated with VIC model parameters is generally lower than the uncertainties from
618 precipitation inputs. Su et al. (2022) indicated that changes in the RB are within 8% when
619 B_inf ranges from 0.05 to 0.4, D2 ranges from 0.5 to 3.0 m, and the changes in NSE are
620 generally within 0.1. Therefore, high-density hydrometeorological observations are expected
621 to better constrain the model and further improve the description of hydrological responses to
622 climate and spatiotemporal changes in glacier/snow.
623
624 Uncertainties are introduced by different representation of physical processes in hydrological

https://doi.org/10.5194/hess-2024-11
Preprint. Discussion started: 23 January 2024


Hydrology and Earth System Sciences
Discussions

625 model, especially the snow and glacier melt simulation in high-mountainous basins. Existing
626 studies used different definitions of runoff composition. For example, Lutz et al. (2014) and
627 Khanal et al. (2021) divided total runoff into four compositions: rainfall runoff, snow melt,
628 glacier melt and baseflow. Some studies also further divided the glacier melt into ice melt and
629 supraglacial snowmelt (Armstrong et al. 2018; Wang et al. 2021). In this study, we divided
630 total runoff into rainfall runoff, snow melt and glacier runoff. Baseflow is a relatively stable
631 streamflow composition, and it plays an important role in sustaining surface water flow,
632 especially for the winter half-year when surface water availability is limited. The VIC model
633 accounts for baseflow (https://vic.readthedocs.io/en/master/), which is comprised of three soil
634 layers to represent the rapid dynamics of soil moisture movement during storm events
635 (surface runoff) and the slower deep inter-storm response in the bottom layer (baseflow).
636 Figure S16 shows mean annual contribution and annual variation contribution of rainfall
637 runoff, snowmelt, glacier runoff and baseflow to total runoff. The baseflow contribution was
638 relatively stable, and it only contributed of 4% to total runoff in the NX basin since 1971.
639 Wang et al. (2022) quantified the contribution of baseflow by the water and energy budget-
640 based distributed hydrological model (WEB-DHM), and suggested mean annual baseflow
641 contributed of 3.3% to total runoff. However, different model structures to represent baseflow
642 processes may also result in uncertainties. In addition, the effect of climate change on the
643 baseflow in the YZ basin remains uncertain mainly due to the generally poor understanding of
644 mountain aquifers. Detailed study of infiltration and recharge processes, aquifer

https://doi.org/10.5194/hess-2024-11
Preprint. Discussion started: 23 January 2024

645 characteristics, and flow pathways needs to be a focus of future research to predict how
646 baseflow will respond to the changes in climate and cryosphere.
647
648 The representation of glacier melting processes introduces substantial uncertainties in model
649 simulations. The accuracy of distinguishing between debris-free and debris-covered glacier
650 extents at the basin scale critically influences the simulated contribution of glacier runoff.
651 Currently, the differentiation between these two glacier surface types relies on elevation
652 constraints. However, due to the observation in these two glacier surface types, the DDFs
653 were set to the same value in the debris-free and debris-covered glacier. To address this
654 pivotal issue, additional glacier observations encompassing both surface types, coupled with
655 high-quality remote sensing mapping, would solve this key issue. This approach holds the
656 potential to refine distinctions between debris-free and debris-covered glaciers, thereby
657 enhancing the precision of model simulations concerning glacier melting processes.
658
659 Another key issue is the restricted comprehension of the effect of snow and ice sublimation on
660 glacier runoff. Sublimation can potentially be an important component of the high-altitude
661 water balance in the Himalayan region (Lutz et al., 2016). Sublimation was mostly calculated
662 based on gauge measurement and estimated using an elevation-dependent potential
663 sublimation function (Lutz et al., 2016; Khanal et al., 2021; Stigter et al. 2018). Stigter et al.
664 (2018) suggested that the fraction of snowfall sublimation may be much higher than 21% at

https://doi.org/10.5194/hess-2024-11
Preprint. Discussion started: 23 January 2024


Hydrology and Earth System Sciences
Discussions

665 wind-exposed locations in the Himalayan region. Lutz et al. (2016) and Khanal et al. (2021)
666 proposed that snow sublimation accounts for approximately 10% in the UI basin and 2%–3%
667 in the YZ basin. Furthermore, the impact of snow sublimation diminished as a result of a
668 smaller fraction of precipitation falling as snow with ongoing warming (Khanal et al., 2021).
669 Yang et al. (2013) investigated mass balance of a maritime glacier on the YZ basin of the
670 southeast TP during 2005–2010, and indicated that the mass loss by way of
671 sublimation/evaporation was quite negligible (about -0.07 m/yr).

672

673 **5.2 Implications for Water Management**

674 Understanding the regional runoff characteristics and changes carries significant implications
675 for water management in the river basin. Firstly, variations in runoff regimes and changes
676 across sub-basins in the YZ necessitate informed policy decisions on local water management.
677 In the LS and NX basins, increased flows from April to September, related to increased
678 rainfall and earlier snowmelt peaks, can alleviate irrigation water shortages during the initial
679 stages of the growing season in drought-prone periods (Immerzeel et al., 2010). Conversely,
680 the NX-BXK basin experiences decreased flows primarily from September to May due to
681 decreased rainfall and snowmelt, demanding attention from hydrological authorities to
682 address potential on water security and availability. Furthermore, climate changes have led to
683 increased natural hazards associated with the cryosphere, such as glacier lake outburst floods
684 and glacier collapses. Notably, a glacier collapse on 16th and 29th October 2018 blocked the

https://doi.org/10.5194/hess-2024-11
Preprint. Discussion started: 23 January 2024

main course of the river, causing a dam-breaching flood in the downstream sub-basin of the YZ, threatening the lives of over 20,000 people in Mainling County and Medog County, respectively (Chen et al., 2020; An et al., 2021; Zhao et al., 2022). Therefore, it is crucial to further investigate the effects of glacier change on hydrological processes and prioritize early warning of cryosphere-related natural hazards in the NX-BXK, which accounts for about 65% of the total glacier area and approximately 52% of the runoff in the YZ basin.

Second, the decrease in runoff since 1998, coupled with an anticipated increase in future runoff, may lead to alterations in extreme floods and hydrological drought risks. This underscores the need for informed policy decisions to protect downstream populations from the adverse effects of these events. The Yarlung-Brahmaputra basin is one of the world's largest and most populated regions, supporting approximately 70 million people across China, India, Bangladesh, and Bhutan countries (Pradhan et al., 2021). Increased flood risks during the wet season and drought risks in the dry season are particularly relevant for human safety and agricultural production in both the upper and downstream basins of the YZ (Liu et al., 2018; Gao et al., 2019). Downstream regions, especially vast agricultural areas along main rivers and in the delta's floodplain, may experience higher floodwater levels from upper regions, posing risks of reduced productivity and crop failure (Hoang et al., 2016). Therefore, urgent implementation of mitigation and adaptation strategies is necessary to address water security problems arising from flood or drought hazards in this basin.

https://doi.org/10.5194/hess-2024-11
Preprint. Discussion started: 23 January 2024


Hydrology and Earth System Sciences
Discussions

705

706 **6 Conclusions**

707 This study comprehensively investigates runoff composition, flow changes, and their
708 attribution across six sub-basins in the YZ for 1971–2020, with a particular focus on the
709 comparison between the NX and NX-BXK using a newly generated precipitation dataset and
710 a well-validated large-scale VIC-Glacier model with observed streamflow at eight
711 hydrological stations, glacier mass balance data at two sites, and satellite-based glacier and
712 snow cover estimates. The study also assesses the future evolution of annual and seasonal
713 total water availability, as well as glacier runoff and snowmelt contributions, using an
714 ensemble of multiple GCMs from CMIP6 under two SSPs. The key findings are summarized
715 as follows:

716

717 1. Large regional differences in runoff regimes were observed in the YZ basin for 1971–2020.
718 The NX-BXK contributed 52% to total runoff at the Pasighat outlet of the YZ basin, followed
719 by the YC-NX (25%), LS (10%), and other sub-basins. While rain-induced runoff dominated
720 the entire YZ (59%–72%), glacier runoff played a more important role in annual total runoff
721 in downstream sub-basins (16%–19%), particularly in summer (23%–35%).

722

723 2. Regional differences in runoff changes were identified in the YZ basin. Annual runoff
724 generally increased (8–19 mm/10yr) during 1971–2020 in all sub-basins of the NX basin, but

https://doi.org/10.5194/hess-2024-11
Preprint. Discussion started: 23 January 2024

a significant decrease is noted in the NX-BXK sub-basin (-9.4 mm/10yr). Total runoff trends reversed after 1998 for all sub-basins of the YZ, with increasing trends during 1971–1997 and decreasing trends during 1998–2020, influenced by changes in summer rainfall runoff due to atmospheric moisture and teleconnection indices (PDO, ENSO, and AMO). Glacier runoff mitigated the decreasing contribution from rainfall since 1998, exhibiting an increased effect on water supply.

3. Total runoff will consistently increase (27–100 mm/10yr) across the sub-basins through the 21st century, with increases of 7–27 mm/10yr in NX and 34–100 mm/10yr in NX-BXK under two SSPs, resulting from increased rainfall runoff and minor effect of increased snowmelt and glacier runoff. Relative to the 1971–2000 mean, a decrease of about -6% to -14% is expected in the first half of the 21st century (2021–2050), followed by a consistent increase (6%–32%) in the second half (2071–2100).

Acknowledgments

This study was financially supported by the National Natural Science Foundation of China (42201140), a project funded by the China Postdoctoral Science Foundation (2022M723256), and the Second Tibetan Plateau Scientific Expedition and Research (STEP) Program (2019QZKK0201). We extend our gratitude to Daqing Yang, Ying Li, Qikai Sun and Tinghai Ou for their constructive suggestions.

https://doi.org/10.5194/hess-2024-11
Preprint. Discussion started: 23 January 2024

Data availability

All the data utilized in this study is presented in the main text.

Author Contributions

He Sun: Conceptualization, Formal analysis, Investigation, Methodology, Resources, Visualization, Funding acquisition, Writing draft. Tandong Yao: Writing (review and editing). Fengge Su: Writing (review and editing). Wei Yang: Editing and provision of glacier mass balance data. Deliang Chen: Writing (review and editing).

Competing interests

The authors declare that they have no known competing financial interests or personal relationships that could have appeared to influence the work reported in this paper.

References

An, B., Wang, W., Yang, W., Wu, G., Guo, Y., Zhu, H., et al., 2021. Process, mechanisms, and early warning of glacier collapse-induced river blocking disasters in the Yarlung Tsangpo Grand Canyon, southeastern Tibetan Plateau, Sci. Total. Environ. 151652. https://doi.org/10.1016/j.scitotenv.2021.151652.

Armstrong, R. L., Rittger, K., Brodzik, M. J., Racoviteanu, A., Barrett, A. P., Khalsa, S. J. S., et al., 2019. Runoff from glacier ice and seasonal snow in High Asia: separating melt water

https://doi.org/10.5194/hess-2024-11
Preprint. Discussion started: 23 January 2024

766 sources in river flow. Reg. Environ. Change. 19, 1249-1261. https://doi.org/10.1007/s10113-
767 018-1429-0.
768 Bahr, D. B., Meier, M. F., Peckham, S. D., 1997. The physical basis of glacier volume-area
769 scaling. J. Geophys. Res. Solid. Earth. 102, 20355-20362. https://doi.org/10.1029/97jb01696.
770 Barnett, T. P., Adam, J. C., Lettenmaier, D. P., 2005. Potential impacts of a warming climate
771 on water availability in snow-dominated regions. Nature. 438, 303-309.
772 https://doi.org/10.1038/nature04141.
773 Chen, C., Zhang, L., Xiao, T., He, J., 2020. Barrier lake bursting and flood routing in the
774 Yarlung Tsangpo Grand Canyon in October 2018. J. Hydrol. 583.
775 https://doi.org/10.1016/j.jhydrol.2020.124603.
776 Chen, X., Long, D., Hong, Y., Zeng, C., Yan, D., 2017. Improved modeling of snow and
777 glacier melting by a progressive two-stage calibration strategy with GRACE and multisource
778 data: How snow and glacier meltwater contributes to the runoff of the Upper Brahmaputra
779 River basin?, Water. Resour. Res. 53, 2431–2466. https://doi.org/10.1002/2016WR019656.
780 Cui, T., Li, Y., Yang, L., Nan, Y., Li, K., Tudaji, M., et al., 2023. Non-monotonic changes in
781 Asian Water Towers' streamflow at increasing warming levels. Nat. Commun. 14(1), 1176.
782 https://doi.org/10.1038/s41467-023-36804-6.
783 Cuo, L., Zhang, Y., 2017. Spatial patterns of wet season precipitation vertical gradients on the
784 Tibetan Plateau and the surroundings. Sci. Rep. 7, 5057. https://doi.org/10.1038/s41598-017-
785 05345-6.

https://doi.org/10.5194/hess-2024-11
Preprint. Discussion started: 23 January 2024

786 Cuo, L., Li, N., Liu, Z., Ding, J., Liang, L., Zhang, Y., Gong, T., 2019. Warming and human
787 activities induced changes in the Yarlung Tsangpo basin of the Tibetan plateau and their
788 influences on streamflow. J. Hydrol-Reg. Stud. 25, 100625.
789 https://doi.org/10.1016/j.ejrh.2019.100625.
790 Dahri, Z. H., Ludwig, F., Moors, E., Ahmad, S., Ahmad, B., Shoaib, M., et al., 2021. Spatio‐
791 temporal evaluation of gridded precipitation products for the high‐altitude Indus basin. Int. J.
792 Climatol. 41, 4283-4306. https://doi.org/10.1002/joc.7073.
793 Duethmann, D., Peters, J., Blume, T., Vorogushyn, S., & Güntner, A., 2014. The value of
794 satellite-derived snow cover images for calibrating a hydrological model in snow-dominated
795 catchments in Central Asia. Water. Resources. Res. 50, 2002-2021. https://doi.org/
796 10.1002/2013WR014382.
797 Gao, C., Liu, L., Ma, D., He, K., Xu, Y. P., 2019. Assessing responses of hydrological
798 processes to climate change over the southeastern Tibetan Plateau based on resampling of
799 future climate scenarios. Sci. Total. Environ. 664, 737-752.
800 https://doi.org/10.1016/j.scitotenv.2019.02.013.
801 Gu, H., Xu, Y. P., Liu, L., Xie, J., Wang, L., Pan, S., Guo, Y., 2023. Seasonal catchment
802 memory of high mountain rivers in the Tibetan Plateau. Nat. Commun. 14(1), 3173.
803 https://doi.org/10.1038/s41467-023-38966-9.
804 Hoang, L. P., Lauri, H., Kummu, M., Koponen, J., van Vliet, M. T. H., Supit, I., Leemans, R.,
805 et al., 2016. Mekong River flow and hydrological extremes under climate change. Hydrol.

806 Earth Syst. Sci. 20, 3027-3041.https://doi.org/10.5194/hess-20-3027-2016.

807 Hock, R., 2003. Temperature index melt modelling in mountain areas, J. Hydrol. 282, 104-115.

808 https://doi.org/10.1016/s0022-1694(03)00257-9.

809 Jost, G., Moore, R. D., Menounos, B., Wheate, R., 2012. Quantifying the contribution of

810 glacier runoff to streamflow in the upper Columbia River Basin, Canada. Hydrol. Earth. Syst.

811 Sc. 16, 849-860. https://doi.org/10.5194/hess-16-849-2012.

812 Kan, B., Su, F., Xu, B., Xie, Y., Li, J., Zhang, H., 2018. Generation of High Mountain

813 Precipitation and Temperature Data for a Quantitative Assessment of Flow Regime in the

814 Upper Yarkant Basin in the Karakoram J. Geophys. Res. Atmos. 123, 8462-8486.

815 https://doi.org/10.1029/2017jd028055.

816 Khanal, S., Lutz, A. F., Kraaijenbrink, P. D., van den Hurk, B., Yao, T., & Immerzeel, W. W.,

817 2021. Variable 21st century climate change response for rivers in High Mountain Asia at

818 seasonal to decadal time scales. Water. Resources. Res. e2020WR029266.

819 https://doi.org/10.1029/2020WR029266.

820 Li, C., Su, F., Yang, D., Tong, K., Meng, F., Kan, B., 2018. Spatiotemporal variation of snow

821 cover over the Tibetan Plateau based on MODIS snow product, 2001-2014. Int. J. Climatol.

822 38, 708-728, https://doi.org/10.1002/joc.5204.

823 Liang, X., Lettenmaie, D. P., Wood, E. F., Burges, S. J., 1994. A simple hydrologically based

824 model of land-surface water and energy fluxes. J. Geophys. Res. Atmos. 99, 14415–14428.

825 https://doi.org/10.1029/94jd00483.

https://doi.org/10.5194/hess-2024-11
Preprint. Discussion started: 23 January 2024


Hydrology and Earth System Sciences
Discussions

826 Liang, X., Lettenmaier, D. P., Wood, E. F., 1996. One-dimensional statistical dynamic
827 representation of subgrid spatial variability of precipitation in the two-layer variable
828 infiltration capacity model. J. Geophys. Res. Atmos. 101, 21403-21422.
829 https://doi.org/10.1029/96jd01448.
830 Liu, L., Gu, H., Xie, J., Xu, Y. P., 2020. How well do the ERA-Interim, ERA-5, GLDAS-2.1
831 and NCEP-R2 reanalysis datasets represent daily air temperature over the Tibetan Plateau? Int.
832 J. Climatol. 41, 1484-1505. https://doi.org/10.1002/joc.6867.
833 Liu, L., Pan, S. L., Bai, Z. X., Xu, Y. P., 2018. Potential application of hydrological ensemble
834 prediction in forecasting flood and its components over the Yarlung Zangbo River Basin,
835 China. Hydrol. Earth. Syst. Sci. Discuss. 1-33, https://doi.org/10.5194/hess-2018-179.
836 Liu, S., Sun, W., Shen, Y., Li, G., 2003. Glacier changes since the Little Ice Age maximum in
837 the western Qilian Shan, northwest China, and consequences of glacier runoff for water
838 supply, J. Glaciol. 49, 117-124, https://doi.org/10.3189/172756503781830926.
839 Liu, Y., Wu, G., Hong, J., Dong, B., Duan, A., Bao, Q., Zhou, L., 2012. Revisiting Asian
840 monsoon formation and change associated with Tibetan Plateau forcing: II. Chang. Clim.
841 Dynam., 39, 1183-1195, https://doi.org/10.1007/s00382-012-1335-y.
842 Lutz, A. F., Immerzeel, W. W., Kraaijenbrink, P. D., Shrestha, A. B., Bierkens, M. F., 2016.
843 Climate Change Impacts on the Upper Indus Hydrology: Sources, Shifts and Extremes, PLoS
844 One, 11, e0165630. https://doi.org/10.1371/journal.pone.0165630.
845 Lutz, A. F., Immerzeel, W. W., Shrestha, A. B., Bierkens, M. F. P., 2014. Consistent increase

https://doi.org/10.5194/hess-2024-11
Preprint. Discussion started: 23 January 2024


Hydrology and Earth System Sciences
Discussions

846 in High Asia's runoff due to increasing glacier melt and precipitation. Nat. Clim. Change. 4,
847 587-592. https://doi.org/10.1038/nclimate2237.
848 Meng, F. C., Su, F. G., Li, Y., Tong, K., 2019. Changes in Terrestrial Water Storage During
849 2003-2014 and Possible Causes in Tibetan Plateau. J. Geophys. Res. Atmos. 124, 2909-2931.
850 https://doi.org/10.1029/2018jd029552.
851 Meng, F., Su, F., Sun, H., Huang, J., Li, C., 2023. Divergent runoff regime revealed by
852 hydrological simulations with corrected precipitation in the upper Indus. J. Hydrol. 626,
853 130315. https://doi.org/10.1016/j.jhydrol.2023.130315.
854 Miao, L., Li, S., Zhang, F., Chen, T., Shan, Y., and Zhang, Y., 2020. Future Drought in the Dry
855 Lands of Asia Under the 1.5 and 2.0 °C Warming Scenarios. Earth's Future. 8,
856 e2019EF001337. https://doi.org/10.1029/2019ef001337.
857 Nan, Y., Tian, L., He, Z., Tian, F., Shao, L., 2021. The value of water isotope data on
858 improving process understanding in a glacierized catchment on the Tibetan Plateau. Hydrol.
859 Earth Syst. Sci., 25(6), 3653-3673. https://doi.org/10.5194/hess-25-3653-2021.
860 Niu, Q., Liu, L., Heng, J., Li, H., Xu, Z., 2020. A Multi-Index Evaluation of Drought
861 Characteristics in the Yarlung Zangbo River Basin of Tibetan Plateau, Southwest China. Front.
862 Earth. Sc. 8, 213. https://doi.org/10.3389/feart.2020.00213.
863 Pradhan, N. S., Das, P. J., Gupta, N., Shrestha, A. B., 2021. Sustainable Management Options
864 for Healthy Rivers in South Asia: The Case of Brahmaputra, Sustainability, 13, 1987.
865 https://doi.org/10.3390/su13031087.

https://doi.org/10.5194/hess-2024-11
Preprint. Discussion started: 23 January 2024


Hydrology and Earth System Sciences
Discussions

866 Pritchard, H. D., 2019. Asia's shrinking glaciers protect large populations from drought stress.
867 Nature, 569, 649-654. https://doi.org/10.1038/s41586-019-1240-1.
868 Qi, W., Liu, J., Chen, D., 2018. Evaluations and Improvements of GLDAS2.0 and GLDAS2.1
869 Forcing Data's Applicability for Basin Scale Hydrological Simulations in the Tibetan Plateau.
870 J. Geophys. Res. Atmos. 123, 13,128-113,148. https://doi.org/10.1029/2018JD029116.
871 Radić, V., Hock, R., 2010. Regional and global volumes of glaciers derived from statistical
872 upscaling of glacier inventory data. J. Geophys. Res-earth. 115.
873 https://doi.org/10.1029/2009JF001373.
874 Shi, X. G., Wood, A. W., Lettenmaier, D. P., 2008. How Essential is Hydrologic Model
875 Calibration to Seasonal Streamflow Forecasting? J. Hydrometeorol. 9(6), 1350–1363.
876 https://doi.org/10.1175/2008JHM1001.1.
877 Stigter, E. E., M. Litt, J. F. Steiner, P. N. J. Bonekamp, J. M. Shea, M. F. P. Bierkens, et al.,
878 2018. The Importance of Snow Sublimation on a Himalayan Glacier. Front. Earth. Sci. 6, 108.
879 https://doi.org/10.3389/feart.2018.00108.
880 Su, F., Hong, Y., Lettenmaier, D. P., 2008. Evaluation of TRMM Multisatellite Precipitation
881 Analysis (TMPA) and Its Utility in Hydrologic Prediction in the La Plata Basin, J.
882 Hydrometeorol. 9, 622-640, https://doi.org/10.1175/2007jhm944.1.
883 Su, F., Pritchard, H. D., Yao, T., Huang, J., Ou, T., Meng, F., et al., 2022. Contrasting Fate of
884 Western Third Pole's Water Resources Under 21st Century Climate Change. Earth's Future. 10.
885 https://doi.org/10.1029/2022ef002776.

https://doi.org/10.5194/hess-2024-11
Preprint. Discussion started: 23 January 2024


Hydrology and Earth System Sciences
Discussions

886 Su, F., Zhang, L., Ou, T., Chen, D., Yao, T., Tong, K., et al., 2016. Hydrological response to
887 future climate changes for the major upstream river basins in the Tibetan Plateau. Glob. Planet.
888 Chang. 136, 82-95. https://doi.org/10.1016/j.gloplacha.2015.10.012.
889 Sun, H. Su, F., 2020. Precipitation correction and reconstruction for streamflow simulation
890 based on 262 rain gauges in the upper Brahmaputra of southern Tibetan Plateau. J. Hydrol.
891 590. https://doi.org/10.1016/j.jhydrol.2020.125484.
892 Sun, H., Su, F., He, Z., Ou, T., Chen, D., Li, Z., et al., 2021. Hydrological evaluation of high-
893 resolution precipitation estimates from the WRF model in the Third Pole river basins. J.
894 Hydrometeorol., https://doi.org/10.1175/jhm-d-20-0272.1.
895 Sun, H., Yao, T., Su, F., He, Z., Tang, G., Li, N., et al., 2022. Corrected ERA5 precipitation by
896 machine learning significantly improved flow simulations for the Third Pole basins. J.
897 Hydrometeorol. 23. https://doi.org/10.1175/JHM-D-22-0015.1.
898 Sun, H., Yao, T., Su, F., Ou, T., He, Z., Tang, G., et al., 2024. Increased glacier melt enhances
899 future extreme floods in the southern Tibetan Plateau. Adv. Climate. Change. Res.
900 Tang, Q., Lan, C., Su, F., Liu, X., Sun, H., Ding, J. et al., 2019. Streamflow change on the
901 Qinghai-Tibet Plateau and its impacts. Chin. Sci. Bull. 64(27), 2807–2821.
902 https://doi.org/10.1360/TB-2019-0141.
903 Tong, K., Su, F., Xu, B., 2016. Quantifying the contribution of glacier meltwater in the
904 expansion of the largest lake in Tibet. J. Geophys. Res. Atmos. 121, 11158–11173.
905 https://doi.org/10.1002/2016jd025424.

https://doi.org/10.5194/hess-2024-11
Preprint. Discussion started: 23 January 2024


Hydrology and Earth System Sciences
Discussions

906 Tong, K., Su, F., Yang, D., Zhang, L., Hao, Z., 2014. Tibetan Plateau precipitation as depicted
907 by gauge observations, reanalyses and satellite retrievals. Int. J. Climatol. 34, 265-285.
908 https://doi.org/10.1002/joc.3682.
909 Wang, A., Zeng, X., 2012. Evaluation of multireanalysis products with in situ observations
910 over the Tibetan Plateau. J. Geophys. Res. Atmos. 117(D5).
911 https://doi.org/10.1029/2011jd016553.
912 Wang, A., Wang, Y., Su, B., Kundzewicz, Z. W., Tao, H., Wen, S., et al., 2020. Comparison of
913 Changing Population Exposure to Droughts in River Basins of the Tarim and the Indus.
914 Earth's Future. 8. https://doi.org/10.1029/2019ef001448.
915 Wang, L., Cuo, L., Luo, D., Su, F., Ye, Q., Yao, T., et al., 2022: Observing multi-sphere
916 hydrological changes in the largest river basin of the Tibetan Plateau. Bull. Am. Meteorol. Soc.
917 103(6), E1595-E1620. https://doi.org/10.1175/BAMS-D-21-0217.1.
918 Wang, X., Luo, Y., Sun, L., & Shafeeque, M., 2021. Different climate factors contributing for
919 runoff increases in the high glacierized tributaries of Tarim River Basin, China. J. Hydrol-reg.
920 stud. 36, 100845. https://doi.org/10.1016/j.ejrh.2021.100845.
921 Wang, Y., Wang, L., Zhou, J., Yao, T., Yang, W., Zhong, X., et al., 2021. Vanishing glaciers at
922 southeast Tibetan Plateau have not offset the declining runoff at Yarlung Zangbo. Geophys.
923 Res. Lett. 48, e2021GL094651. https://doi.org/10.1029/2021gl094651.
924 Wu, G., Duan, A., 2008. Weakening Trend in the Atmospheric Heat Source over the Tibetan
925 Plateau during Recent Decades. Part I: Observations. J. Clim. 21, 3149-3164.

https://doi.org/10.5194/hess-2024-11
Preprint. Discussion started: 23 January 2024

926 https://doi.org/10.1175/2007jcli1912.1.

927 Wood, A. W., 2002. Long-range experimental hydrologic forecasting for the eastern United
928 States. J. Geophys. Res. Atmos. 107(D20), ACL-6. https://doi.org/1029/2001JD000659.

929 Wood, A. W., Leung, L. R., Sridhar, V., Lettenmaier, D. P., 2004. Hydrologic Implications of
930 Dynamical and Statistical Approaches to Downscaling Climate Model Outputs. Clim. Change.
931 62, 189-216. https://doi.org/10.1023/B:CLIM.0000013685.99609.9e.

932 Wu, G., Duan, A., 2009. Weakening Trend in the Atmospheric Heat Source over the Tibetan
933 Plateau during Recent Decades. Part II: Connection with Climate Warming. J. Clim. 22, 4197-
934 4212. https://doi.org/10.1175/2009jcli2699.1.

935 Yang, W., Guo, X., Yao, T., Yang, K., Zhao, L., Li, S., et al., 2011. Summertime surface
936 energy budget and ablation modeling in the ablation zone of a maritime Tibetan glacier. J.
937 Geophys. Res. Atmos. 116. https://doi.org/10.1029/2010jd015183.

938 Yang, W., Yao, T., Guo, X., Zhu, M., Li, S., Kattel, D. B., 2013. Mass balance of a maritime
939 glacier on the southeast Tibetan Plateau and its climatic sensitivity. J. Geophys. Res. Atmos.
940 118, 9579-9594. https://doi.org/10.1002/jgrd.50760.

941 Yang, Y., Gao, D., Li, B., 1989. Study on the moisture passage on the lower reaches of the
942 Yarlung Zangbo river, Sci. China (Series B) 32, 580-593.

943 Yang, Z., Zhuo, M., Lu, H., Ma, P., Zhou, K., 2014b. Characteristics of precipitation variation
944 and its effects on runoff in the Yarlung Zangbo River basin during 1961–2010. Journal of
945 Glaciology and Geocryology, 36, 166-172 (in chinese).

https://doi.org/10.5194/hess-2024-11
Preprint. Discussion started: 23 January 2024

946 Yao, T., Bolch, T., Chen, D., Gao, J., Immerzeel, W., Piao, S., et al., 2022. The imbalance of
947 the Asian water tower. Nat. Rev. Earth. Environ. 3(10), 618-632. https://doi.org/s43017-022-
948 00299-4.
949 Yao, T., Thompson, L., Yang, W., Yu, W., Gao, Y., Guo, X., et al., 2012. Different glacier
950 status with atmospheric circulations in Tibetan Plateau and surroundings, Nat. Clim. Chang. 2,
951 663-667. https://doi.org/10.1038/nclimate1580.
952 Yao, T. 2004. Recent glacial retreat in High Asia in China and its impact on water resource in
953 Northwest China, Sci. China (Series D). 47, 1065. https://doi.org/10.1360/03yd0256.
954 Zhang, L., Su, F., Yang, D., Hao, Z., Tong, K., 2013. Discharge regime and simulation for the
955 upstream of major rivers over Tibetan Plateau, J. Geophys. Res. Atmos. 118, 8500-8518.
956 https://doi.org/10.1002/jgrd.50665.
957 Zhao, C., Yang, W., Westoby, M., An, B., Wu, G., Wang, W., et al., 2022. Brief
958 communication: An approximately 50 Mm³ ice-rock avalanche on 22
959 March 2021 in the Sedongpu valley, southeastern Tibetan Plateau. The Cryosphere. 16, 1333-
960 1340, https://doi.org/10.5194/tc-16-1333-2022.
961 Zhao, Q., Ding, Y., Wang, J., Gao, H., Zhang, S., Zhao, C., et al., 2019. Projecting climate
962 change impacts on hydrological processes on the Tibetan Plateau with model calibration
963 against the Glacier Inventory Data and observed streamflow. J. Hydrol. 573, 60-81.
964 https://doi.org/10.1016/j.jhydrol.2019.03.043.
965 Zhong, L., Ma, Y., Fu, Y., Pan, X., Hu, W., Su, Z., et al., 2014. Assessment of soil water

https://doi.org/10.5194/hess-2024-11
Preprint. Discussion started: 23 January 2024

966 deficit for the middle reaches of Yarlung-Zangbo River from optical and passive microwave

967 images. Remote. Sens. Environ. 142, 1-8. https://doi.org/10.1016/j.rse.2013.11.008.

968

https://doi.org/10.5194/hess-2024-11
Preprint. Discussion started: 23 January 2024


Hydrology and Earth System Sciences
Discussions

Captions:

https://doi.org/10.5194/hess-2024-11
Preprint. Discussion started: 23 January 2024


Hydrology and Earth System Sciences
Discussions

https://doi.org/10.5194/hess-2024-11
Preprint. Discussion started: 23 January 2024

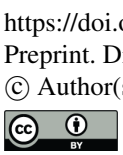

Hydrology and Earth System Sciences
Discussions
Open Access
EGU

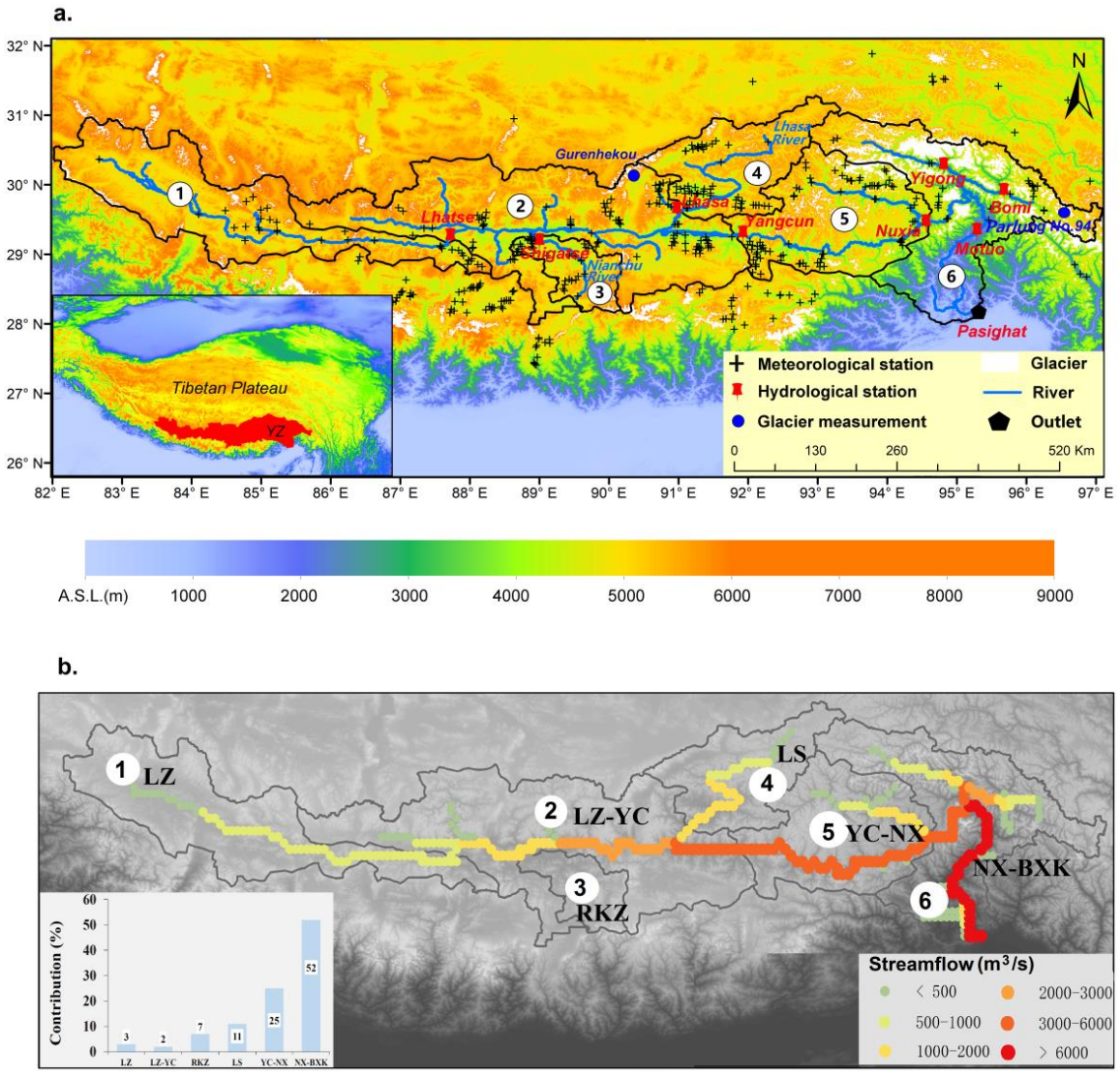

Figure 1. (a) Location and topography of the Yarlung Zangbo (YZ) river basin. Sub-basins, numbered 1 to 6, represent Lhatse (LZ), Lhatse-Yangcun (LZ-YC), Shigatse (RKZ), Lhasa (LS), Yangcun-Nuxia (YC-NX), and Nuxia-Pasighat (NX-BXK), respectively. (b) Spatial pattern of average annual streamflow for 1971–2020 in the YZ basin. The lower histogram shows the mean annual streamflow contribution from each sub-basin to the Pasighat outlet for 1971–2020 in the YZ.

https://doi.org/10.5194/hess-2024-11
Preprint. Discussion started: 23 January 2024

Hydrology and Earth System Sciences
Discussions

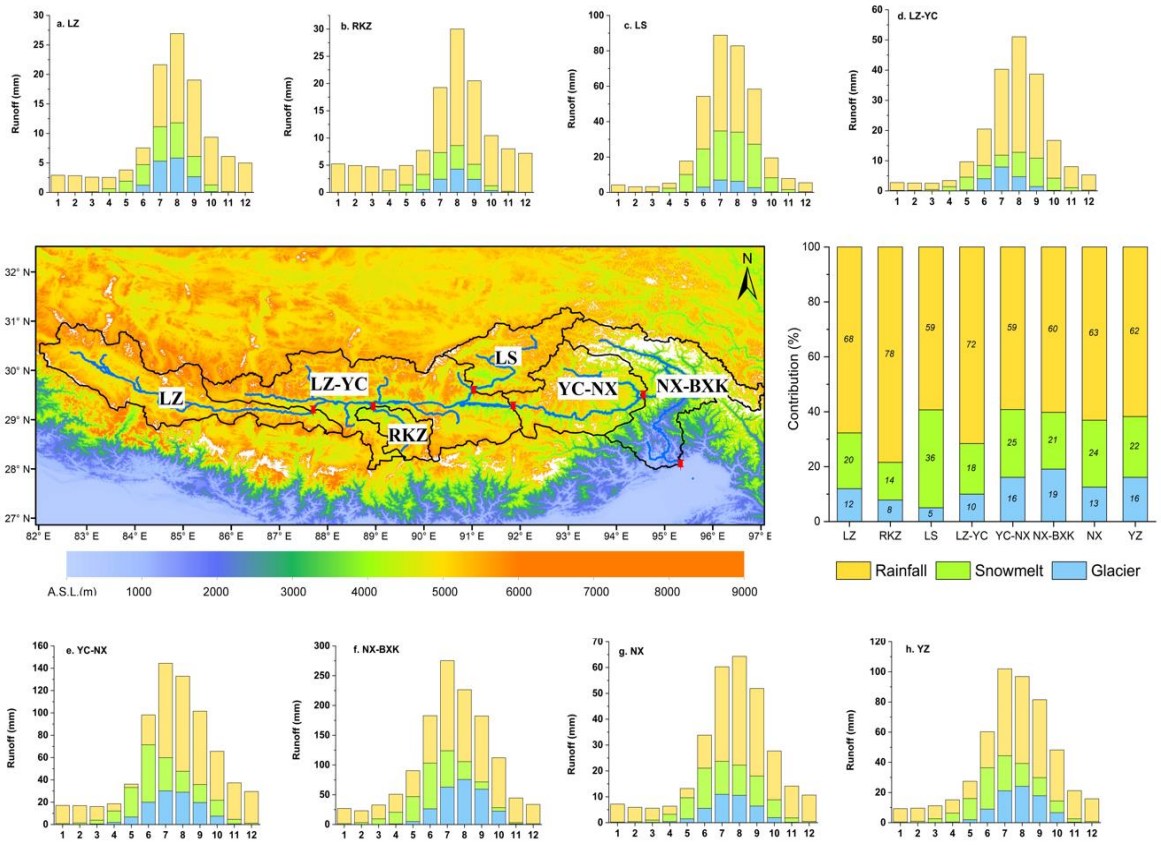

Figure 2. Mean monthly simulated rainfall, snowmelt, and glacier runoff, along with their contribution to total annual runoff in the YZ and its sub-basins for 1971–2020.

https://doi.org/10.5194/hess-2024-11
Preprint. Discussion started: 23 January 2024

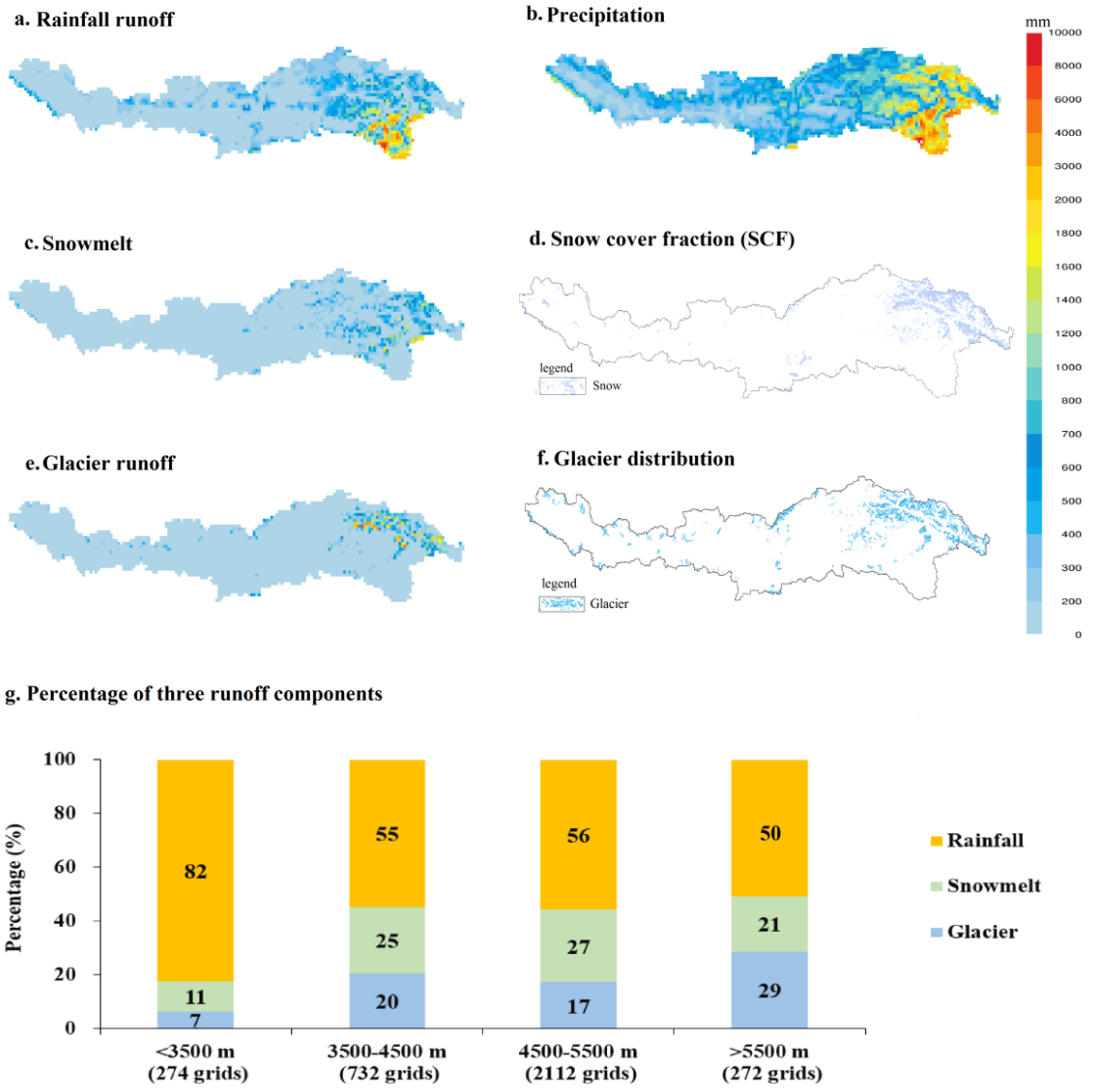

Figure 3. Spatial pattern of average annual rainfall runoff (a), snowmelt (c), glacier runoff (e), and precipitation (b) for 1971–2020 in the YZ basin. The spatial pattern of average annual snow cover fraction (SCF, d) for 2001–2019 and glacier distribution in the YZ basin. Percentage (%) of three runoff components (rainfall, snowmelt, and glacier runoff) at four elevation bands in the YZ basin, with the number in parentheses indicating the number of 10-km grids in each elevation band.

Hydrology and Earth System Sciences
Discussions
Open Access

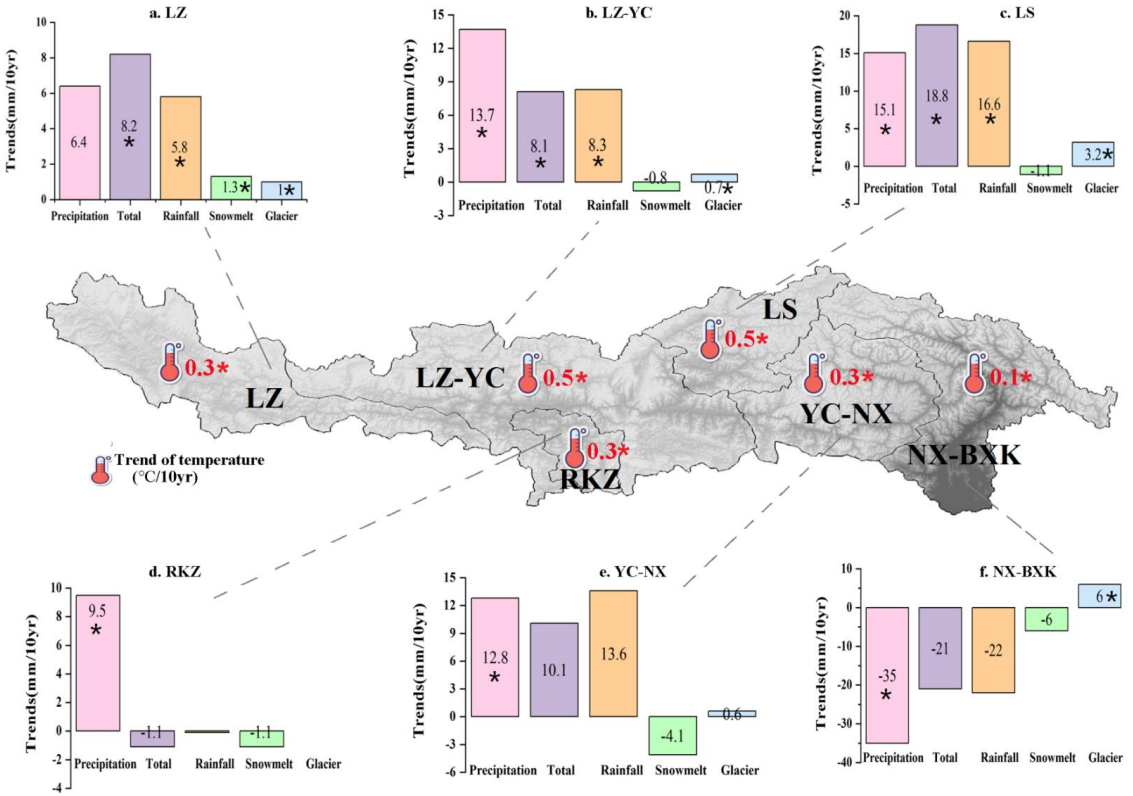

Figure 4. Annual trends in precipitation (mm/10yr), temperature (°C/10yr), total runoff (mm/10yr), and three runoff components (rainfall, glacier, and snowmelt runoff, mm/10yr) in the six sub-basins for 1971–2020, respectively. Asterisks indicate the 95% significance level.

https://doi.org/10.5194/hess-2024-11
Preprint. Discussion started: 23 January 2024

https://doi.org/10.5194/hess-2024-11
Preprint. Discussion started: 23 January 2024

Hydrology and Earth System Sciences
Discussions
Open Access
EGU

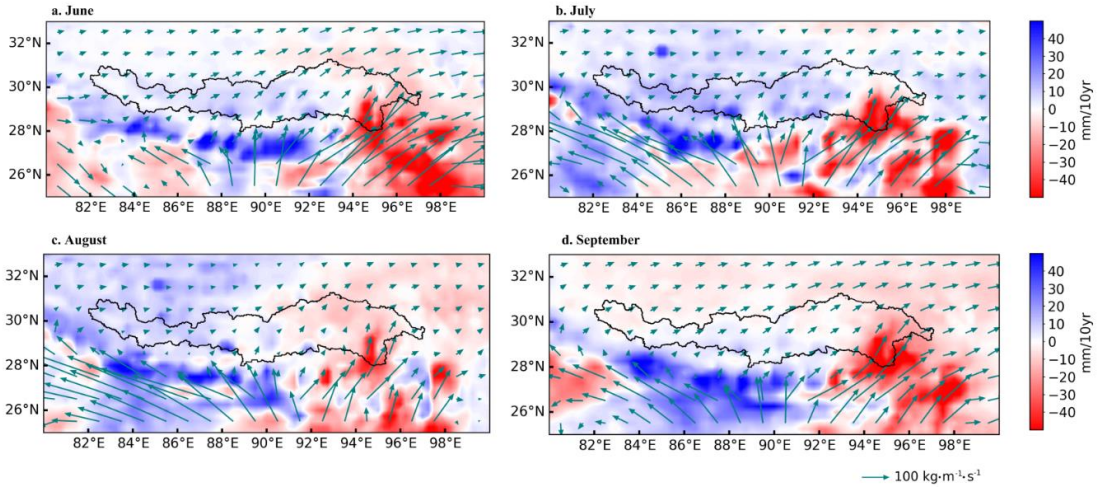

Figure 5. Mean monthly vertical integral of atmospheric moisture budget (mm) in June, July, August, and September from the ERA5 data across the Yarlung Zangbo river basin for 1971–2020 (indicated by colors). Arrows represent the directions of the vertical integral of water vapor flux ($kg \cdot m^{-1} \cdot s^{-1}$).

https://doi.org/10.5194/hess-2024-11
Preprint. Discussion started: 23 January 2024

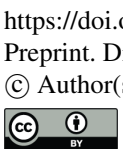

Hydrology and Earth System Sciences
Discussions

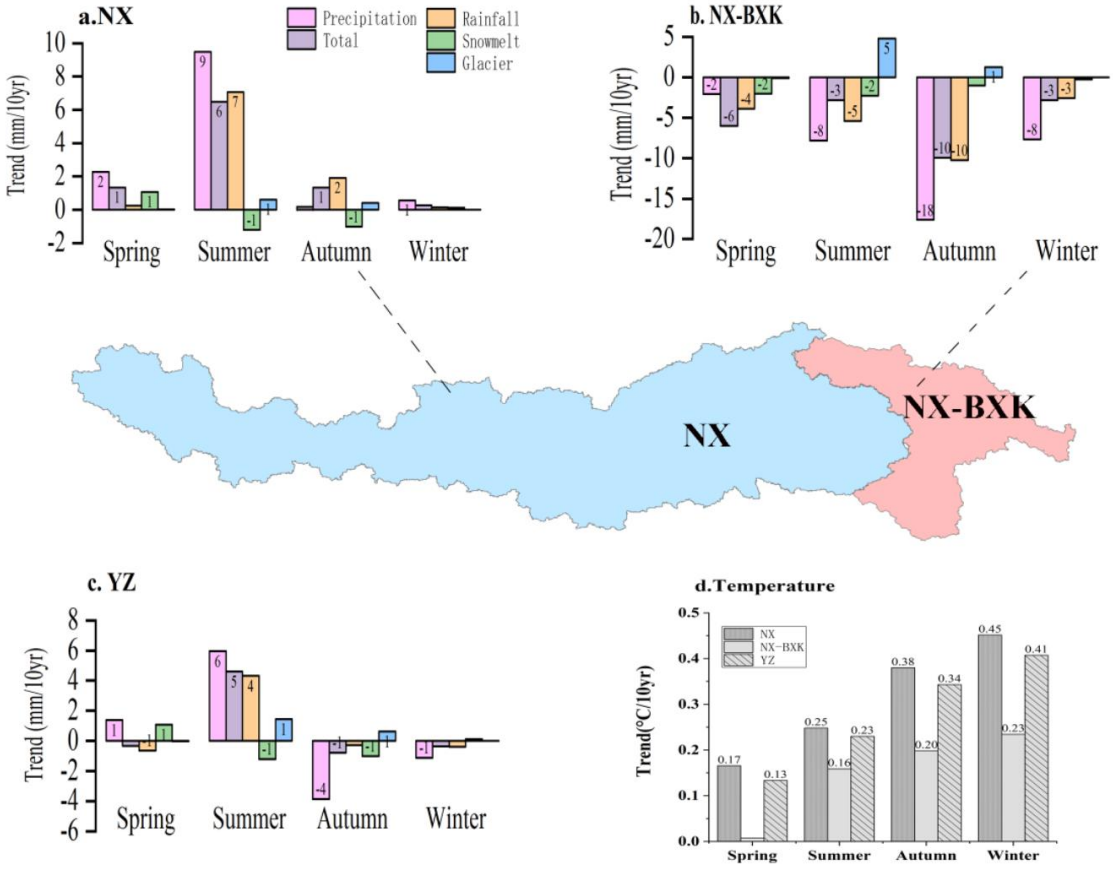

Figure 6. Seasonal trends in precipitation (mm/10yr), temperature (°C/10yr), total runoff (mm/10yr), and three runoff components (rainfall, glacier, and snowmelt runoff, mm/10yr) in the YZ and its sub-basins for 1971–2020, respectively.

https://doi.org/10.5194/hess-2024-11
Preprint. Discussion started: 23 January 2024

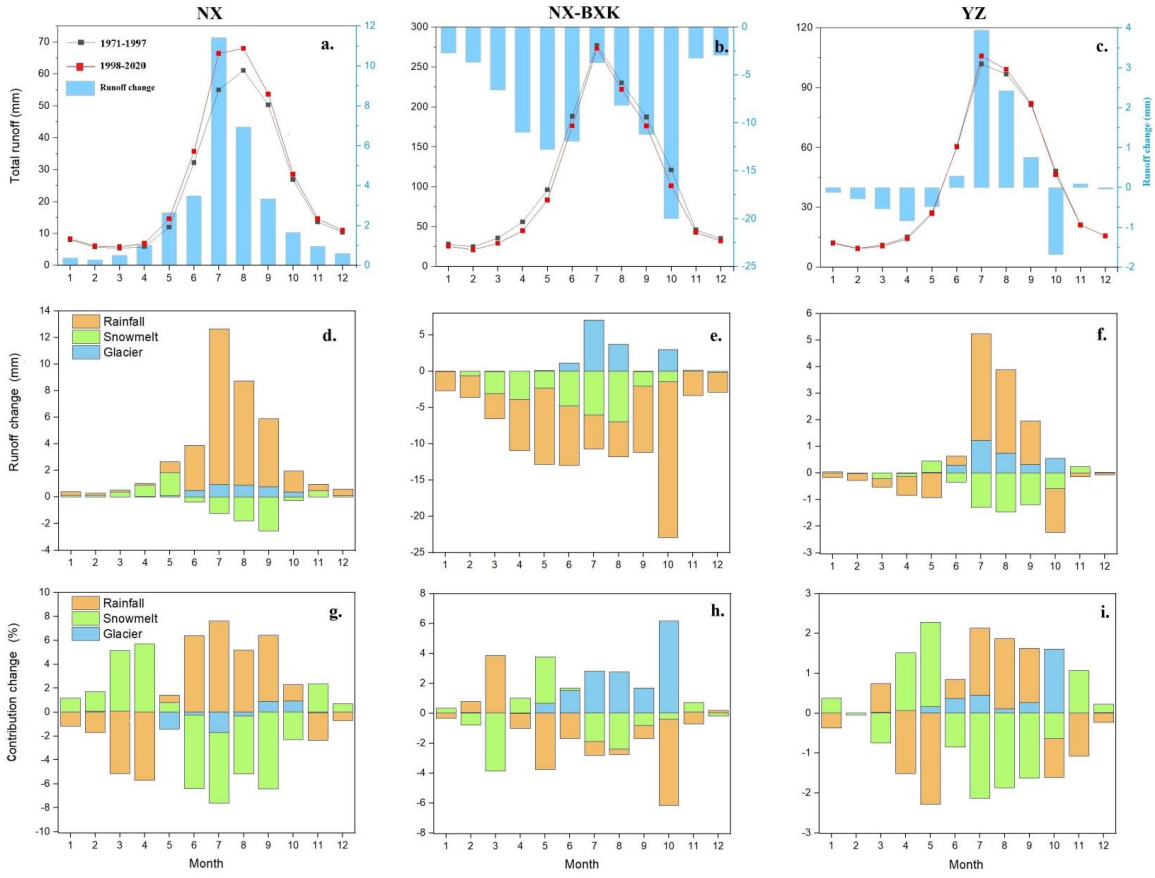

Figure 7. Changes in (a–c) mean monthly total runoff, (d–f) three components, and (g–i) their contributions to total runoff for the period 1998–2020 relative to the period 1971–1997 in the entire YZ basin and its NX and NX-BXK sub-basins.

https://doi.org/10.5194/hess-2024-11
Preprint. Discussion started: 23 January 2024

Hydrology and Earth System Sciences
Discussions

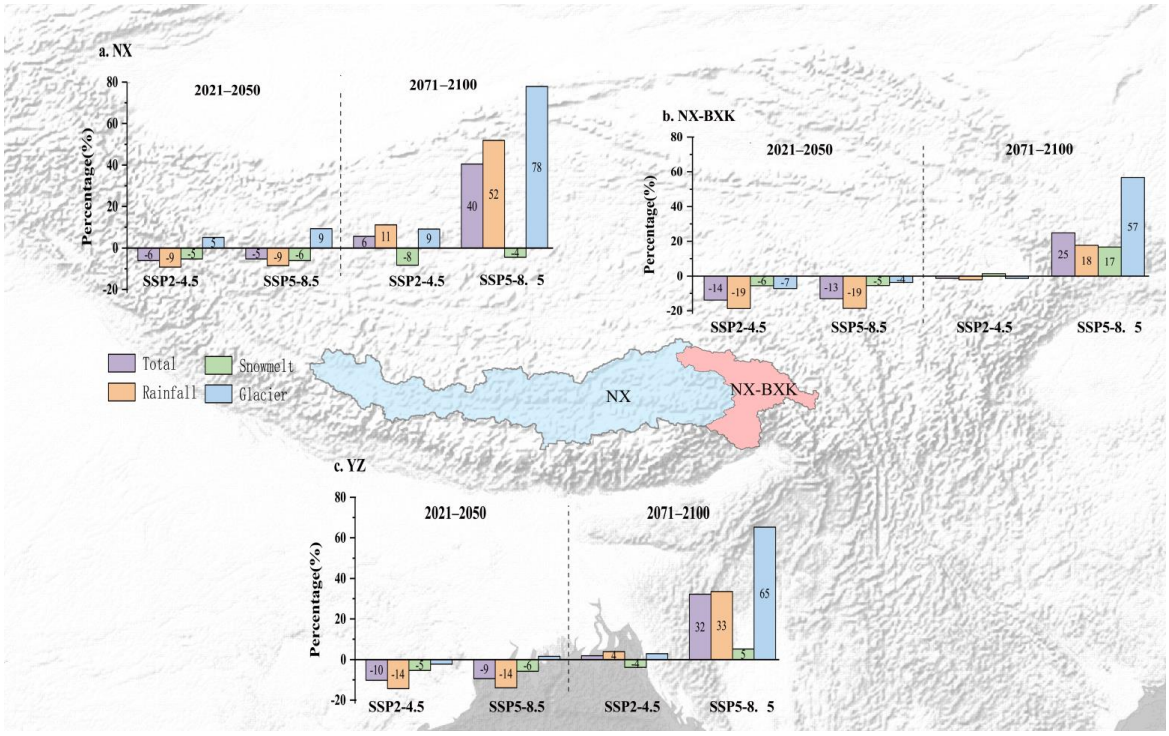

Figure 8. Projected changes (%) in the mean annual total runoff, and three runoff components (rainfall, glacier, and snowmelt) in 2021–2050 and 2071–2100, respectively, relative to 1971–2000 under the two SSPs in the YZ and its NX and NX-BXK sub-basins.

https://doi.org/10.5194/hess-2024-11
Preprint. Discussion started: 23 January 2024

Hydrology and Earth System Sciences
Discussions

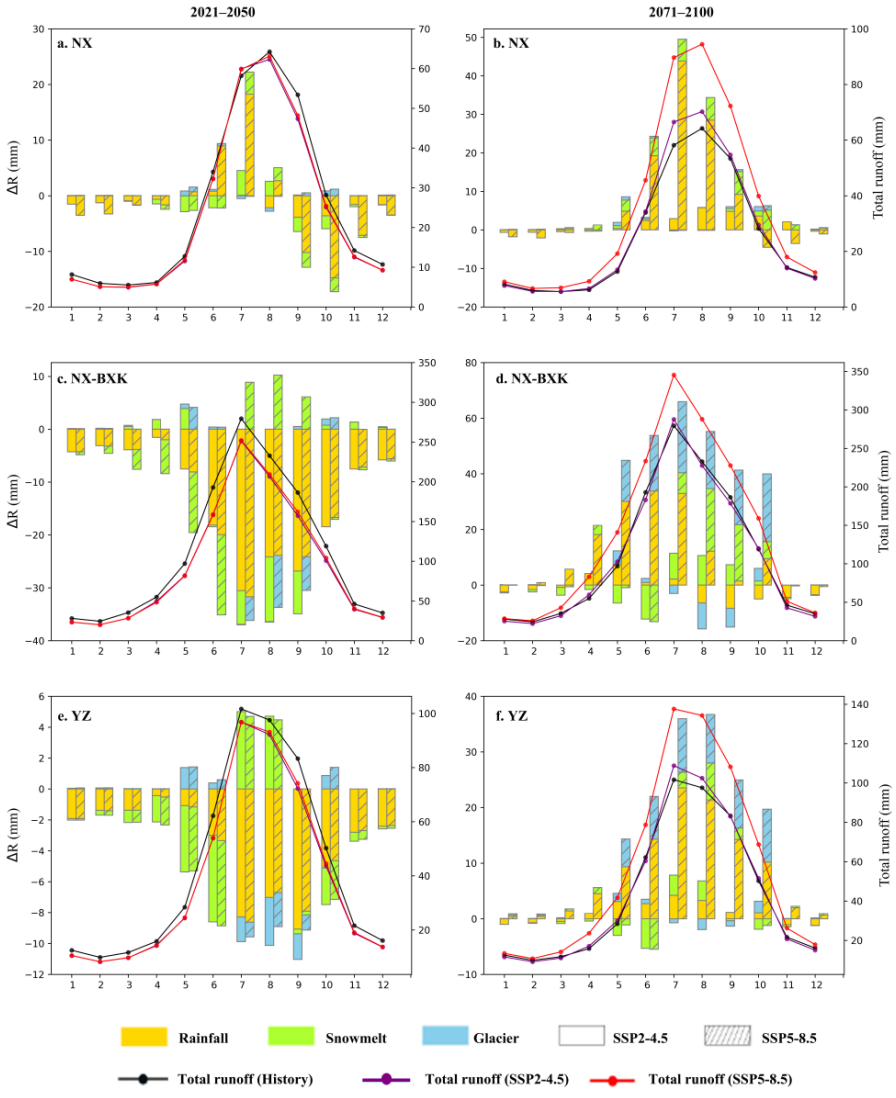

Figure 9. Monthly average of total runoff (mm) in 1971–2000, 2021–2050, and 2071–2100 and the change (mm) in their runoff components relative to 1971–2000. Dotted solid lines represent simulated mean monthly total runoff in three periods. Bar plots indicate the mean seasonal changes in rainfall, snowmelt, and glacier runoff in 2021–2050 and 2071–2100 relative to 1971–2000, based on the ensemble means of 10 hydrological simulations under the two SSPs in the YZ and its NX and NX-BXK sub-basins.

https://doi.org/10.5194/hess-2024-11
Preprint. Discussion started: 23 January 2024

Hydrology and Earth System Sciences
Discussions

Table 1. Summary of relevant studies on simulated runoff component contributions in the YZ basin.

Basin	Runoff contribution (%)			Period	Method	Precipitation Data	References
	Glacier	Snowmelt	Rainfall				
NX	11.6	23	65.4	1961–1999	VIC+DD	Corrected CMA data	Zhang et al. (2013)
	16	9	59	1998–2007	SPHY+DD	APHRODITE	Lutz et al. 2014
	15	27.3	57.7	1971–2000	VIC+DD	Corrected CMA data	Su et al. (2016)
	9.9	10.6	79.5	2003–2014	CREST	CGDPA, TMPA	Chen et al. (2017)
	5.5	23.1	71.4	1971–2010	VIC+DD	Interpolated CMA data	Zhao et al. (2019)
	13.9	23.8	62.3	1980–2000	VIC+DD	Reconstructed data	Sun and Su (2020)
	1.8	13.2	62.1	1985–2014	SPHY+DD	ERA5	Khanal et al. (2021)
	18.4	22	69.6	2001–2010	isoGSM	CMFD	Nan et al. (2021)
	3.5–7.2	16.6–22.3	—	1981–2019	WEB-DHM	Reconstructed data	Wang et al. (2021)
NX-BXK	45.3	15.1	39.6	1980–2000	VIC+DD	Reconstructed data	Sun and Su (2020)
	5.7–8.2	7.2–7.8	—	1981–2019	WEB-DHM	Reconstructed data	Wang et al. (2021)
YZ	32.7	18.4	48.9	1980–2000	VIC+DD	Reconstructed data	Sun and Su (2020)
	5.5	17.2	73.3	1981–2019	WEB-DHM	Reconstructed data	Wang et al. (2021)

Note: VIC+DD=The Variable Infiltration Capacity (VIC) linked with a degree-day glacier melting model; SPHY+DD=The Spatial Processes in Hydrology (SPHY) linked with a degree-day glacier melting model; CREST=Coupled Routing and Excess Storage model; isoGSM=Scripps global spectral model with water isotopes incorporated; WEB-DHM= Water and energy budget-based distributed hydrological model; CMFD= China Meteorological Forcing Dataset.

https://doi.org/10.5194/hess-2024-11
Preprint. Discussion started: 23 January 2024

Hydrology and Earth System Sciences
Discussions
Open Access
EGU

Table 2. Characteristics of the six sub-basins in the Yarlung Zangbo River

		LZ	LZ-YC	RKZ	LS	YC-NX	NX-BXK	YZ
Outlet		Lhatse	Yangcun	Shigatse	Lhasa	Nuxia	Pasighat	Pasighat
Hydrological station	Name	Lhatse	Yangcun	Shigatse	Lhasa	Nuxia	Motuo	—
	Latitude (°N)	29.05	29.28	29.25	29.63	29.47	29.32	—
	Longitude (°E)	87.38	91.88	88.88	91.15	94.57	95.29	—
Drainage area (km^2)		50553	71926	11064	26235	41770	51507	253,055
Basin average elevation (m)		5370	4767	5353	5272	4937	3711	4901
Mean annual precipitation (mm) *		283	417	361	564	939	1465	774
Mean annual temperature (°C) *		-2.91	0.24	1.73	-1.28	0.97	1.21	-0.2
Glacier area (km^2)		809	640	134	257	1174	5259	8273
Glacier coverage (%) **		1.60	0.89	1.21	0.98	2.81	10.21	3.27
Snow cover area (km^2) ***		7876	7344	772	6055	10129	16467	48643
Snow cover fraction (%) ***		15.58	10.21	6.98	23.08	24.25	31.97	19.22

*The periods of precipitation and temperature data are from 1961 to 2020 (Sun et al., 2022).

**Glacier data are from the first China Glacier Inventory, http://westdc.westgis.ac.cn/glacier.

***snow cover area and snow cover fraction data are from the MODIS 10CM (2001–2019), https://nsidc.org/data

https://doi.org/10.5194/hess-2024-11
Preprint. Discussion started: 23 January 2024

Hydrology and Earth System Sciences
Discussions

Table 3. Values of the first (D1, m), the second soil depth (D2, m) and degree-day factor (DDF), and the Nash-Sutcliffe Efficiency (NSE) and Relative Bias (RB, %) of the simulated monthly streamflow with the Variable Infiltration Capacity (VIC)-Glacier model relative to the observation for the eight hydrological stations.

Sub-basin	Hydrological station	D1(m)	D2(m)	DDF ($mm°C^{-1}$ day^{-1})	Calibration		Validation	
					NSE	RB (%)	NSE	RB (%)
LZ	LZ	0.1	0.7	10.97	0.85	2.1	0.81	1.8
LZ-YC	YC	0.1	0.7	10.97	0.83	3	0.81	1.6
RKZ	RKZ	0.1	0.9	10.97	0.84	-4	0.71	-8
LS	LS	0.1	0.7	9.2	0.84	-2	0.82	-2
YC-NX	NX	0.1	1	6.8	0.86	-4	0.86	-5
NX-	YG	0.1	1	6.5	0.82	-8	0.83	-5
BXK	BM	0.1	1	6.5	0.83	-6	0.83	-5
	MT	0.1	1	6.5	0.71	6	0.73	5

https://doi.org/10.5194/hess-2024-11
Preprint. Discussion started: 23 January 2024

Hydrology and Earth System Sciences
Discussions

Table 4. Trends in precipitation, temperature, total runoff, and three runoff components and their contributions to total runoff in the YZ and its NX and NX-BXK sub-basins for different periods. Asterisks indicate the 95% confidence level.

Basin		NX			NX-BXK			YZ		
Period		1971–2020	1971–1997	1998–2020	1971–2020	1971–1997	1998–2020	1971–2020	1971–1997	1998–2020
Precipitation (mm/10yr)		11.7 *	2.9	-6.9	-35 *	52	-16.4	2.1	8.3	-8.8
Temperature (℃/10yr)		0.4 *	0.2 *	0.3 *	0.1 *	0.1	0.3 *	0.3 *	0.2 *	0.3 *
Runoff (mm/10yr)	Total	9.4 *	1.1	-3.3	-21	48.1	-0.3	3.1	8.9	-2.7
	Glacier	1.1 *	0.6	0.7	6.0 *	0.1	16.1	2.0 *	0.1	3.9
	Snowmelt	-1	0.5	-3.4	-6	20.6 *	5.7	-1.9 *	4.6 *	-1.5
	Rainfall	9.4 *	0.9	-0.6	-22	27.6	-22.1	3.0	4.9	-5.0
Contribution (%/10yr)	Glacier	-0.1	-0.2	0.3	0.8 *	-0.7	1.2	0.3	-0.4	0.8
	Snowmelt	-1.1 *	0.3	-0.8	-0.1	0.9	0.3	-0.5 *	0.6	-0.3
	Rainfall	1.1 *	-0.1	0.6	-0.7 *	-0.3	-1.6 *	0.2	-0.2	-0.5

https://doi.org/10.5194/hess-2024-11
Preprint. Discussion started: 23 January 2024

Hydrology and Earth System Sciences
Discussions

Table 5. Trends of projected annual precipitation (mm/10 yr), temperature (°C/10 yr), and total runoff and runoff components (mm per decade) from 10 GCMs for 1971–2000, 2021–2050, and 2071–2100 under the two SSPs in the YZ and its two sub-basins (The uncertainties are indicated with one standard deviation).

		NX	NX-BXK	YZ
SSP2-4.5 2021–2050	Total runoff	6.84±4.9	52.65±22.41	16.15±7.37
	Rainfall runoff	5.53±3.97	29.99±15.43	10.54±5.73
	Snowmelt	-0.43±1.0	9.24±6.88	1.54±1.71
	Glacier runoff	1.68±1.32	13.41±6.91	4.07±2.38
	Precipitation	4.98±8.96	31.87±27.85	10.4±11.59
	Temperature	0.43±0.16	0.42±0.12	0.43±0.15
SSP5-8.5 2021–2050	Total runoff	16.22±6.78	59.34±28.23	24.99±10.59
	Rainfall runoff	11.9±5.75	31.2±22.06	15.82±8.69
	Snowmelt	1.35±1.05	9.53±5.65	3.01±1.88
	Glacier runoff	2.98±0.54	18.61±3.77	6.16±1.06
	Precipitation	18.02±11.86	32.73±36.08	21.01±16.29
	Temperature	0.66±0.1	0.6±0.09	0.64±0.09
SSP2-4.5 2071–2100	Total runoff	9.23±9.84	25.5±17.35	12.54±10.25
	Rainfall runoff	8.94±8.03	19.67±15.03	11.13±8.83
	Snowmelt	-0.03±1.36	2.12±9.24	0.41±2.01
	Glacier runoff	0.31±1.47	3.71±5.52	1±2.21
	Precipitation	11.36±12.87	23.64±21.36	13.86±12.59
	Temperature	0.32±0.2	0.27±0.15	0.31±0.19
SSP5-8.5 2071–2100	Total runoff	35.84±23.12	142.1±84.67	57.45±35.38
	Rainfall runoff	33.69±21.52	96.06±53.31	46.37±27.89
	Snowmelt	-3.63±4.7	11.07±6.32	-0.64±3.25
	Glacier runoff	5.78±4.59	34.97±27.18	11.72±9.12
	Precipitation	39.45±25.96	93.83±50.16	50.52±30.66

https://doi.org/10.5194/hess-2024-11
Preprint. Discussion started: 23 January 2024

Hydrology and Earth System Sciences
Discussions

	Temperature	1.01±0.59	0.98±0.57	1±0.58
SSP2-4.5 2021–2100	Total runoff	7.18±2.77	34.09±9.51	12.65±3.91
	Rainfall runoff	7.23±1.89	26.78±6.02	11.21±2.53
	Snowmelt	-0.46±0.56	3.97±1.86	0.44±0.68
	Glacier runoff	0.4±0.58	3.34±2.99	1±1.06
	Precipitation	7.07±2.61	22.51±7.59	10.21±3.02
	Temperature	0.36±0.08	0.34±0.08	0.35±0.08
SSP5-8.5 2021–2100	Total runoff	27.31±10.14	100.85±30.71	42.27±13.82
	Rainfall runoff	21.41±10.14	59.17±18.38	29.09±9.53
	Snowmelt	0.14±0.63	11.96±3.7	2.55±0.96
	Glacier runoff	5.76±2.35	29.73±11.49	10.64±4.18
	Precipitation	25.34±9.39	61.86±23.92	32.77±11.26
	Temperature	0.85±0.17	0.79±0.17	0.84±0.17